

A STUDY OF THE PYRITE-CALC SILICATE RELATIONSHIP
IN THE MENINGIE WELL AREA, OLARY PROVINCE

BY

Lili Haas, B.Sc.

This thesis is submitted as partial fulfilment of the requirements for the Honours Degree of Bachelor of Science in Geology at the University of Adelaide.

November 1980

Copy (2)
DEPARTMENT OF ECONOMIC GEOLOGY,
THE UNIVERSITY OF ADELAIDE,
ADELAIDE,
SOUTH AUSTRALIA

C O N T E N T S

	<u>Page</u>
ABSTRACT	
<u>1. INTRODUCTION</u>	1.
1.1 Location of Study Area	
1.2 Aims of Study	
1.3 Source of Information	
1.4 Previous Investigations	
<u>2. GEOLOGICAL SETTING</u>	3.
2.1 Regional Geology	
2.2 Local Geology	
<u>3. STRATIGRAPHY AND ROCK TYPES</u>	4.
3.1 Introduction	
3.2 Upper Albite Unit	
3.3 Calc Silicate Horizon	
3.3.1 Feldspar-Epidote-Actinolite ± Hornblende	
3.3.2 Feldspar-Augite-Hornblende-Sphene	
3.3.3 Andradite-Hedenbergite-Calcite-Quartz	
3.4 Mixed Horizon	
3.4.1 Feldspar-Calcite-Biotite-Actinolite	
3.4.2 Feldspar-Quartz-Epidote-Actinolite-Mica	
3.4.3 Quartz-Epidote-Calcite-Diopside-Actinolite ± Scapolite	
3.4.4 Quartz-Epidote-Carbonate-Mica ± Feldspar	
3.5 Quartz-Feldspar-Mica Horizon	
3.6 Graphitic Metasiltstone	
<u>4. METAMORPHISM</u>	8.
4.1 Introduction	
4.2 Metamorphic Minerals	
4.3 Metamorphic Textures	
4.4 Original Rock Types	
4.5 Pressure-Temperature Conditions	
<u>5. MINERALIZATION</u>	14.
5.1 Introduction	
5.2 Mineral Types	
5.3 Textures	
5.4 Occurrence	
5.5 Trace Elements in Pyrite	
<u>6. TRACE ELEMENT GEOCHEMISTRY MP1-MP10</u>	19.
6.1 Element-Element Relationships	
6.2 Trace Element-Stratigraphy	
6.3 Trace Element and Lateral Variation	
<u>7. SUMMARY AND CONCLUSIONS</u>	22.
ACKNOWLEDGEMENTS	25.
BIBLIOGRAPHY	26.

C O N T E N T S (Continued)

Fig. 1	-	Regional Location Map
Fig. 2	-	Location Map MP1-MP2, with geochemistry
Fig. 3	-	Stratigraphic Subunits of the Bimba Formation
Fig. 4	-	Pelitic trends in QFM
Fig. 5	-	T - XCO ₂ at 2 kb, 5 kb
Fig. 6	-	TE Geochemistry of MP1-MP10

Plate 1	A, B, C
Plate 2	A, B
Plate 3	A, B, C
Plate 4	A, B, C

Appendix	I	Representative Rock Descriptions
	II	Trace Element Study in Pyrite
	III	Analytical Techniques
	IV	Geochemical Tables
	V	Work Done

* * *

ABSTRACT

The stratiform pyrite mineralization in the Olary Province is hosted by calc silicates, which form part of the metasedimentary sequence in the Olary Province. The calc silicates can be subdivided into three sub units:

- (1) Calc Silicates, which are mainly chemical sedimentation of impure carbonates;
- (2) Mixed Horizon, consisting of interbedded chemical and clastic sedimentation, with possible volcanogenic component;
- (3) Quartz-Feldspar-Mica Horizon, consisting of clastics.

The calc silicates have been metamorphosed at least two times, possibly three. Relict amphibolite facies minerals diopside, scapolite and andradite show mineralogical and textural disequilibrium with the retrograde greenschist facies minerals tremolite, calcite and actinolite. The absence of talc indicates high X_{CO_2} values during the retrograde metamorphism. For $X_{CO_2} = 0.75$, the range of P-T is from 550°C at 2 kb to 650°C at 5 kb.

Textural studies indicate that the pyrite is stratiform and syngenetic. Trace element values, especially Co:Ni ratios suggest that a volcanogenic exhalative component is probable for the mineralization. Cu rich and Zn rich domains are found in the pyrite horizons.

Mineralization appears to have been controlled by the sedimentation of the Mn and Fe rich impure carbonates. Superimposed on this, there has been a gradual change of environments in the basin from oxidizing to reducing, and from a carbonate shelf type facies to a more basinal facies with clastic sedimentation. If the volcanogenic model is real, then the Pyrite-Cu association is typical of shallow water shelf facies, proximal to the volcanic source, whilst the Pyrite-Zn is more basinal and distal from the source.

1. INTRODUCTION

1.1 Location of Study Area

The Study Area lies approximately 20 km north of Olary, between the Old Boolcoomata Homestead and the Meningie South Copper Workings (Fig. 1). The project was suggested by Esso Australia (Minerals Division) Ltd. and Professor Ypma. The area is located within the bounds of the Mulga Dam Exploration Lease held by Esso.

1.2 Aims of the Study

The main aims of the study are:

- (1) Determine the metamorphic effects on the sulphides.
- (2) Investigate the relationship between the sulphides and the metamorphic host.
- (3) Examine Copper, Lead, Zinc and Cobalt abundances in the calc silicates.
- (4) Compare the mineralization - calc silicate relationship in the study area with drill core from Dome Rock.
- (5) Propose a model for sulphide genesis.

1.3 Source of Information

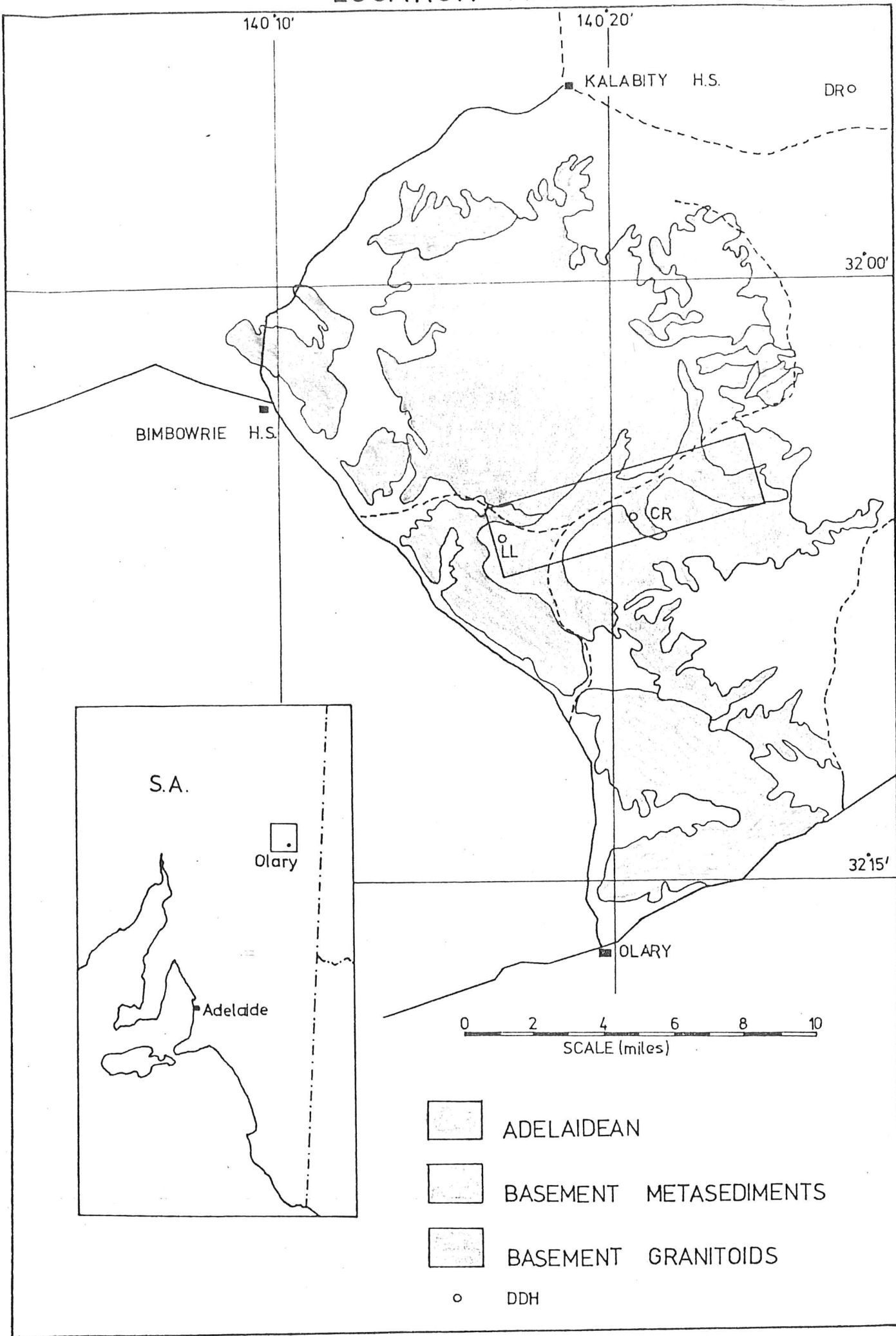
Esso made available percussion samples from ten drill holes in the Meningie Well area, MP1-MP10, (Fig. 2, back pocket), along with logs, trace element geochemistry, maps and gossan analyses. In addition to this several weeks were spent in the field collecting surface samples and identifying field relations of the calc silicates. Additional samples were obtained from drill core available at the Mines Department. The drill holes sampled were Lady Louise (LL1), Cathedral Rock (CR1) and Dome Rock (DR4).

1.4 Previous Investigations

Campana and King (1958) produced a Mines Department Bulletin on the Regional Geology and Mineral Resources of the Olary Province. Previously, Mawson (1911) had investigated chiastolite schists near Mt. Howden and in 1912 undertaken a study of the Broken Hill Region.

LOCATION MAP

fig 1



More recent work by Michelmore (1971) on the geology of copper mineralized areas and by Waterhouse (1971) on the geology of the Ethudna and Walparuta Mine areas has been considered. Petrology and structure of the Wiperaminga Hill was conducted by Parker and Robertson (1972) whilst Cobb and Morris (1970) studied the Weekeroo Amphibolite. Other work by Berry, et al. (1978) on the structure of the Outalpa Area, Gabell (1978) on geochemistry of albitites and Wiltshire (1976) on the geology of the Old Boolcoomata area has been consulted.

More recently, Esso have completed detailed mapping of the Old Boolcoomata - Cathedral Rock - Meningie Well areas at a 1:10.000 scale, and have undertaken an extensive drilling programme in the Meningie Well area.

2. GEOLOGICAL SETTING

2.1 Regional Geology

The Willyama Complex extends from the Broken Hill region to west of Weekeroo Hill, and consists of Lower Proterozoic metasediments and granitoids. Unconformably overlying these are the Adelaidean sediments of Upper Proterozoic age.

In the Olary Province, the Willyama Complex has undergone three stages of metamorphism (Wiltshire, 1975) recognized by field relations. The first and second reaching amphibolite facies at ~1700 m.y. (Compston and Arriens, 1968) and ~1550 m.y. (Compston, et al., 1966) respectively, using comparative dates from the Broken Hill region. The third metamorphic event occurred ~500 m.y. (Compston and Arriens, 1968) and reached greenschist facies. The study area lies within these metasediments which consist largely of schists and gneisses with minor amphibolites, calc silicates and interbedded banded iron formations.

Regionally there has been extensive mineralization with the lead-zinc deposit of Broken Hill in the east and smaller basemetal deposits in the Thackeringa Area. Local occurrences of uranium and REE occur. Copper, tungsten and cobalt have been recorded in association with the calc silicate horizon in the Olary Province.

2.2 Local Geology

The study area occurs as an east-west passage of metasediments between granitoid rocks (Fig. 1). To the north it is bound by Binberrie Hill, a large adamellite intrusive and to the south by Drew Hill, a migmatitic granite gneiss. These granitoids form topographic highs, whilst the metasediments form the lows. These metasediments are extremely weathered and outcrops are poor, making drill core sampling necessary to obtain fresh samples.

The calc silicate horizon, equivalent to the "Ethiudna Calc silicates" (Campana and King, 1958), is the host for the stratabound mineralization in the Olary Province. These calc silicates form good marker horizons between the underlying gneisses and schists and the overlying mica schists (Parker, 1972). They also contain extensive gossaniferous horizons which are stratiform. The stratigraphic bounds for the calc silicates are not always sharply defined due to lateral variation. They show a wide range of mineralogies with tremolite, calcite, diopside and actinolite being predominant.

3. STRATIGRAPHY AND ROCK TYPES

3.1 Introduction

The calc silicates can be divided into three distinctive units, based on mineral associations, with each unit having several sub units (Fig. 3). The lowest stratigraphic unit is called the Calc Silicate Horizon (CS). Overlying this is a Mixed Horizon consisting of calc silicate minerals with interbedded quartz-feldspar-mica horizons. This passes into a Quartz-Feldspar-Mica Horizon (QFM) with no calc silicate influence. Collectively these three units are called the Bimba formation, (field terminology Esso).

Underlying the Bimba Formation is an albite rich horizon called the Upper Albite formation, (field terminology Esso), and overlying it is a Graphitic Metasiltstone (schist). The Bimba Formation is defined between these two horizons.

The stratigraphic change can be seen in all the drill holes sampled, even Dome Rock (DR4) which lies 20 km NNE of the Meningie Well area, and so has been incorporated in the study.

There is a trend for the psammitic-pelitic elements to increase whilst the calc silicate influence decreases from the base of the Bimba Formation to the top. Banding is a strong feature within the Bimba Formation.

3.2 Upper Albite Formation

This unit is fine grained and massive consisting predominantly of albite. Thin bedded magnetite and barite horizons occur within it. Towards the top, the albite unit becomes epidote rich, till it gives way to the calc silicate mineralogy of the lower Bimba Formation. It has been recorded that the Bimba Formation is absent if the Upper Albite unit has also not developed (S. Archibald, pers. comm., 1980).

Work by Gabell (1978) on the Albitites, suggests that they are likely to be altered tuffaceous rocks. However, Wiltshire (1975) proposes that Na metasomatism is the most likely means of formation.

3.3 Calc Silicate Horizon (CS)

This unit has been subdivided into three subunits, which will be considered independently.

* informally

STRATIGRAPHIC SUBUNITS OF THE BIMBA FORMATION

GRAPHITIC METASILTSTONE		
BIMBA FORMATION	QFM HORIZON	Quartz-Feldspar-Mica
	MIXED HORIZON	Quartz-Epidote-Carbonate-Mica ± Feldspar Quartz-Epidote-Calcite-Diopside-Actinolite ± Scapolite Feldspar-Quartz-Epidote-Actinolite-Mica Feldspar-Calcite-Biotite-Actinolite
	CALC SILICATE HORIZON	Andradite-Hedenbergite-Calcite-Quartz Feldspar-Augite-Hornblende-Sphene Feldspar-Epidote-Actinolite ± Hornblende
UPPER ALBITE FORMATION		

3.3.1 Feldspar-Epidote-Actinolite ± Hornblende

This association is banded with either feldspar rich or epidote-actinolite rich bands occurring. The feldspar is high Ab content, Oligoclase-Albite. Some are twinned. Large dusty relict feldspars remain amidst the predominantly recrystallized ones. The amphiboles are large, 3 mm, with apatite, sphene and epidote inclusions. Zoning is evident in the actinolite with the rims being ferroan. Epidote occurs as xenoblastic grains or it may form large skeletal aggregates. Opaques may be associated with this mineral association. In addition opaque stringers occur along the cleavage planes of the actinolite. Sphene and apatite are common accessories.

3.3.2 Feldspar-Augite-Hornblende-Sphene

Feldspar and augite are the main minerals with hornblende rims on the augite occurring as an alteration product. Petrologically it is difficult to determine whether the clinopyroxene is augite or diopside. However, the sphene alteration product along the cleavage planes and the fine grained opaques in the augite-hornblende alteration suggest that it is more likely to be in fact augite. These augites form large grains up to 2 mm in size, which are surrounded by fine grained feldspars ~0.5 mm. The feldspars are dusty, zoned and twinned. This phenocrystic texture may be evidence for an igneous origin. Traces of epidote, apatite and tourmaline occur.

3.3.3 Andradite-Hedenbergite-Calcite-Quartz

This mineral association is rare, and was only found as a segregation in a low stratigraphic position. It consists of coarse grained (Ca,Fe) garnets up to 5 mm in size. These form 60% of the section and were massive, showing no banding. Interstitial to the andradites are medium grained hedenbergite, calcite and quartz. The calcite-hedenbergite contact is lobate, with the calcite as an alteration product of the hedenbergite.

3.4 Mixed Horizon (CS+QFM)

This horizon has been subdivided into four distinct mineral associations. The calc silicate minerals and the quartz-feldspar-mica minerals are inter-layered here resulting in the strong banded appearance of the Bimba Formation.

3.4.1 Feldspar-Calcite-Biotite-Actinolite

Feldspar rich horizons are interlayered with the predominantly marble

rich layers, which may reflect the original sedimentary layering. The micas belong to the phlogopite-biotite series and are ubiquitous. Calcite-biotite-opaque and Calcite-biotite-tremolite (Fe poor actinolite) associations are well developed. Massive, poorly bedded amphibole rich horizons (tremolite-actinolite) also occur, with biotite rimming the amphiboles as an alteration product. Banding in the feldspar rich horizons is distinguished by grain size variation. Accessory sphene is more abundant than apatite.

3.4.2 Feldspar-Quartz-Epidote-Actinolite-Mica

Grain size and compositional variation define the banding in this horizon. A schistosity is developed parallel to the banding which is defined by the preferred orientation of the micas. Quartz-feldspar-mica layers are interbedded with the calc silicate rich horizons. Most of the quartz is recrystallized showing a polygonal texture (Spry, 1969), however large undulose grains with partial subgrain development exist. Similarly, large dusty feldspar relicts occur amongst recrystallized untwinned feldspar grains. The calc silicate bands are dominated by granular aggregates of epidote, which are frequently zoned with clinozoisite cores. Biotite and actinolite are associated with the epidote. Minor chlorite alteration has also occurred. Poikiloblastic actinolites are common in many horizons. Apatite, sphene and zircon are the main accessories with minor amounts of fluorite, garnet and spinel.

3.4.3 Quartz-Epidote-Calcite-Diopside-Actinolite ± Scapolite

Like the previous association, this too shows compositional banding. Fine grained quartz rich layers are interbedded with the calc silicates. Calcite is important here and frequently shows a recrystallized polygonal texture. Large poikiloblastic diopside and scapolite grains up to 2 mm with lobate grain boundaries occur. Actinolite and chlorite alteration rims occur on the diopside indicating a retrograde reaction. Epidote rich horizons are fine grained but may form granular aggregates. Sphene and apatite are the main accessories. Mineralization is frequently associated with these calc silicate horizons.

3.4.4 Quartz-Epidote-Carbonate-Mica ± Feldspar

Carbonate rich layers are interbedded with the quartz-biotite (phlogopite) rich layers to define a compositional layering. The preferred orientation of the micas defines the schistosity. The quartz-biotite (phlogopite) horizons are finer grained than the adjacent calc silicates. Pyrite is associated

with the calcite-siderite-epidote horizons. These coarse grained and recrystallized pyrites show the typical annealed polygonal texture (Vokes, 1969). Siderite forms an intimate relationship with pyrite. Some pyritic mobilization is evident as thin veins extending out from the calc silicate horizons. Fine grained epidote occurs in the quartz-mica horizon and may form a reticulated texture. Chlorite alteration of the micas has occurred. Zircons are abundant in the biotite (phlogopite) rich horizons, sphene is associated with the epidotes and apatite, tourmaline and pyrope occur in trace amounts.

3.5 Quartz-Feldspar-Mica (QFM)

No calc silicate minerals occur in this unit. Banding is evident by the variations in grain size of the quartz and feldspar. The schistosity developed by the micas is parallel to this banding also. Feldspar dominated horizons are recrystallized and untwinned, showing a polygonal texture. However, large dusty relict grains exist which are both zoned and twinned. Extensive sericitization has occurred in these. Feldspar-biotite is a frequent association. These biotites are brown and vary in size depending on abundance. The biotite rich horizons are coarser grained. Large muscovites, up to 5 mm in length, occur in bands. These may be primary. Complete sericitization of lensoidal porphyroblasts, probably sillimanite (Parker, 1972) has been observed. These porphyroblasts are length parallel to the main fabric, and have biotites wrapping around them, indicating metamorphic growth during a previous metamorphism. Apatite, tourmaline, garnet and sphene are the main accessories with fine grained opaque stringers occurring parallel to the banding.

3.6 Graphitic metasiltstone

These rocks consist of quartz, biotite and graphite. Graphite rich and graphite poor horizons define the layering which is also mimicked by the preferred orientation of the biotites. The quartz and biotite are fine grained, less than 0.1 mm, however a few coarser grained horizons occur but these are poor in graphite. This type of observation is typical of graphitic terrains, since graphite seemingly inhibits grain growth during metamorphism. This suggests that the fine grain size of the quartz in graphitic rich horizons is in fact its original clastic size, hence a metasiltstone. The quartz grains are ovoid and length parallel with the layering. The graphite is very fine grained ≤ 0.005 mm and appears as dusty stringers which may form up to 40% of the layer. Apatite is the only accessory.

4. METAMORPHISM

4.1 Introduction

Wiltshire (1975) recognised three metamorphic events in the Old Boolcoomata area. The first two, M1 and M2, reached amphibolite facies and the third, M3, was retrogressive forming greenschist mineral assemblages. He distinguished M1 and M2 on the basis of a relationship between granite gneiss (a product of M1) and an amphibolite intrusion into the gneiss, which had also been metamorphosed to amphibolite facies, therefore suggesting the M2 event. M1 and M2 are frequently difficult to distinguish and are usually treated as a metamorphic episode rather than individual events. The amphibolite facies metamorphisms were responsible for producing partial melts, migmatization and granitic intrusions in the Olary Province. M3 mineral assemblages overprint the high grade assemblages, but a strong mineral and textural disequilibrium exists.

Waterhouse (1971) proposed that diopside, wollastonite, sillimanite and cordierite were typical of the amphibolite grades whilst chloritoid, albite and amphibole were representative of the greenschist facies.

4.2 Metamorphic Minerals

Many of the mineral assemblages are characteristic of the greenschist facies, however relict high grade minerals occur where the retrograde reactions have been incomplete.

Diopside, scapolite and andradite are relict minerals of the amphibolite facies. Scapolite is a high temperature mineral (Orville, 1975) which is stable over a wide range of pressures and temperatures. Similarly, garnet (andradite) forms at temperatures $>500^{\circ}\text{C}$ (Chatterjee, 1967).

Epidote is a metamorphic mineral which characterizes the transition from the Greenschist to the Amphibolite Facies (Deer, Howie and Zussman, 1966). Thus the development of porphyroblastic epidote also represents the amphibolite facies associated with M1 or M2. Epidote is ubiquitous in the calc silicate horizons, and is seemingly stable over a wide range of pressure-temperature conditions.

The hornblende-plagioclase association is typical of the amphibolite facies.

Tremolite, actinolite and calcite are the main retrograde alteration products of the amphibolite facies minerals. They are abundant in the greenschist facies, but show mineralogical and textural disequilibrium here. Minor chlorite alteration also occurs.

Carbonates are abundant with both calcite and siderite recognised. This is a common association in iron rich carbonate environments (Bickle and Powell, 1977). Calcite may be stable to very high P-T conditions especially if X_{CO_2} is high. Thus the presence of calcite alone, does not indicate metamorphic grades, but the texture may indicate metamorphic changes.

Some of the micas associated with the calc silicates belong to the phlogopite-biotite series which is typical of metamorphosed impure limestones.

Quartz and feldspar alone are not suitable for the development of distinctive metamorphic minerals. However, relict sillimanite porphyroblasts occur in a few horizons. These have been completely sericitized.

The main amphibolite and greenschist facies minerals were as follows:

Amphibolite Facies		Greenschist Facies
Diopside	≡	Tremolite and Calcite
Scapolite		
Sillimanite	≡	Sericitized sillimanite
Andradite		
Epidote porphyroblasts	≡	Epidote
Plagioclase-hornblende	≡	Plagioclase-actinolite
		Chlorite
		Actinolite-tremolite-calcite

4.3 Metamorphic Textures

Poorly developed grain boundaries, incomplete recrystallization, zoned grains (epidote, plagioclase) and the relict high grade minerals all suggest a mineralogical and textural disequilibrium.

The most distinctive feature of the Bimba Formation, is the banding. This is defined by the interbedded fine grained quartz-feldspar-mica and the coarser grained calc silicates (Plate 1a). The banding is paralleled by the mica schistosity, by elongation of grains, porphyroblasts, aggregates

and by grain size variation.

This banding may have formed in two ways:

- (1) It may reflect the original compositional variation, i.e. sedimentary layering.
- (2) It may be the result of metamorphic segregation, i.e. metamorphic layering.

The first alternative is more likely for several reasons:

- (a) The schistosity is parallel to the banding and, the gross lithological layering.
- (b) Adjacent bands have diverse compositions, suggesting that it is not simply segregation.
- (c) No metamorphic homogenization has occurred, i.e. the layers show gross chemical differences which probably reflects original variation.
- (d) Graphite, an inert element which is not mobilized during metamorphism, also parallels this banding supporting a sedimentary origin for the layering.
- (e) The banding is continuous on a regional scale, and hence cannot be due to metamorphism, in which the stress field is not always perpendicular to banding.

Epidote develops porphyroblasts, 2 mm, along with calcite and pyrite, to form coarse grained layers. The type of texture that epidote develops depends on abundance. It may form a reticulated network (Plate 1b) or as disseminated xenoblastic grains. Epidote has an intimate association with pyrite (Plate 1c), and is often zoned.

Diopside and scapolite form large poikiloblastic grains, up to 2 mm, with inclusions of quartz, calcite and epidote. Their grain boundaries are lobate indicating textural disequilibrium.

Tremolite and calcite occur as retrograde alteration products of diopside (Plate 2a). Very rarely do the amphiboles (tremolite-actinolite) show well developed grain boundaries. They tend to always be ragged with calcite inclusions. The amphiboles vary in size from fine grained needles, ~0.5, to large poikiloblastic laths up to 4 mm. A strong fabric is not developed in the amphiboles, with most grains randomly orientated.

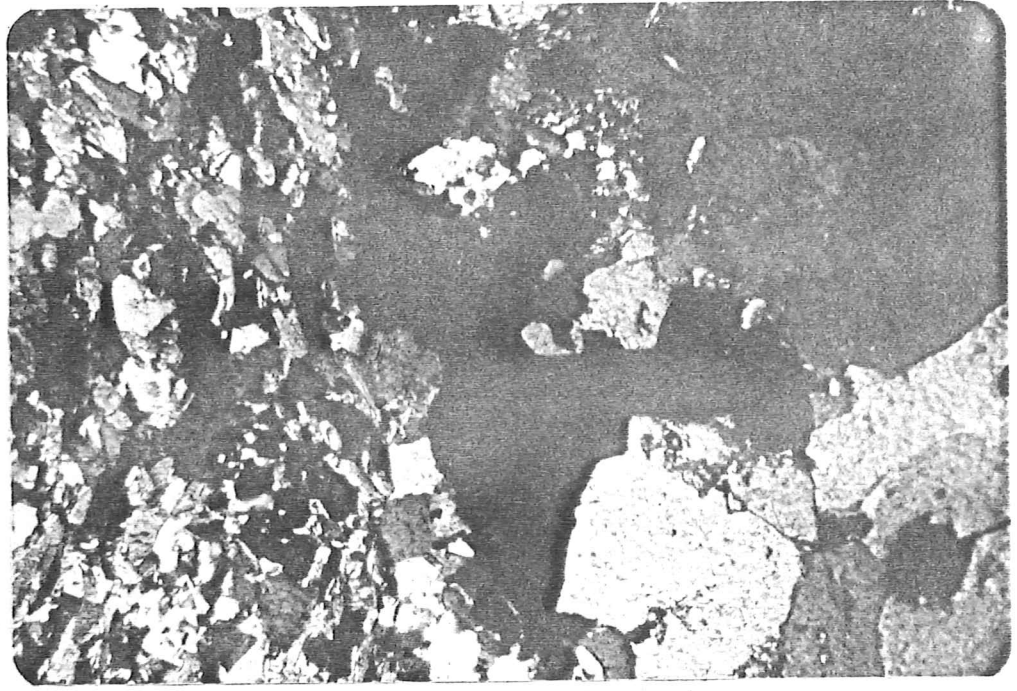
PLATE 1

A. Banded fabric, showing the contrast between fine grained quartz-muscovite-biotite and coarse grained calcite-epidote-opaque. The opaques show an interstitial texture, with some mobilization along calcite cleavages. 764-CR13.

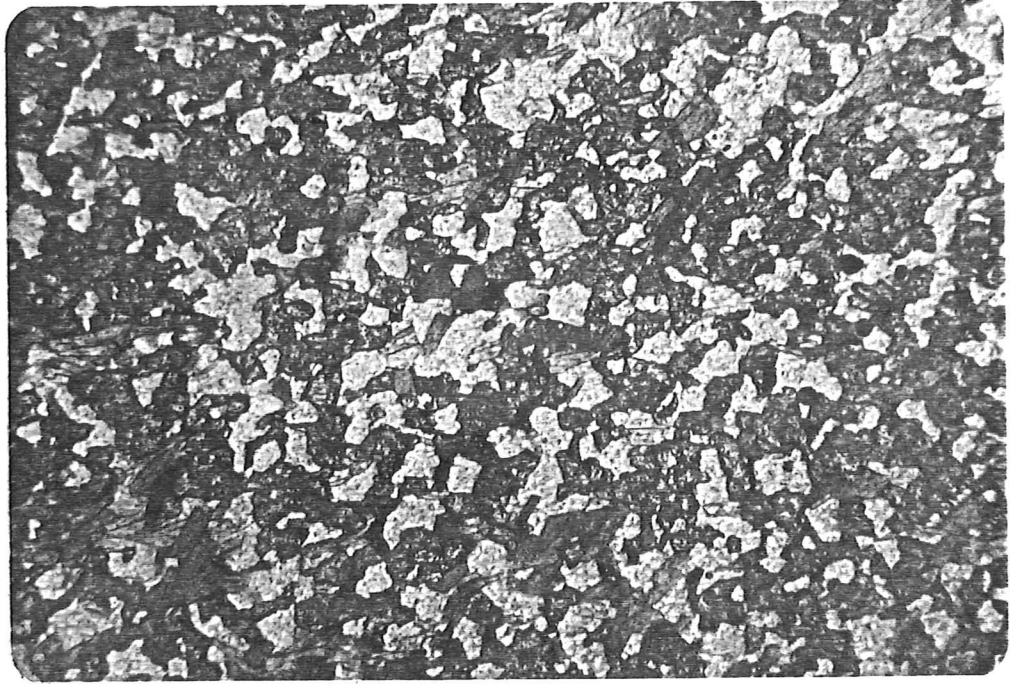
B. Typical reticulate texture of fine grained epidote, associated here with quartz and biotite. 764-CR10.

C. Large ferroan actinolite (A) laths, with opaque stringers along cleavage planes. Pyrite and epidote show an intimate association, with fine grained xenoblastic pyrite in the epidote. 764-LL10.

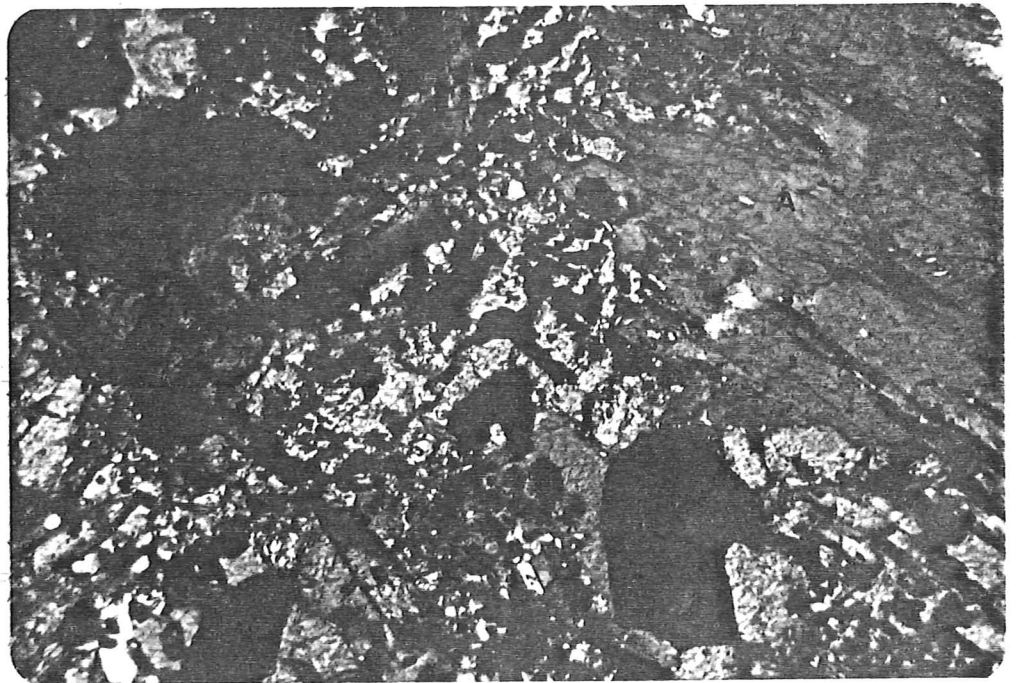
Field of View (F.V.) is 2mm across.



A



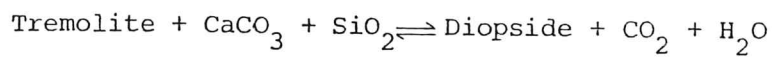
B



C

PLATE 2

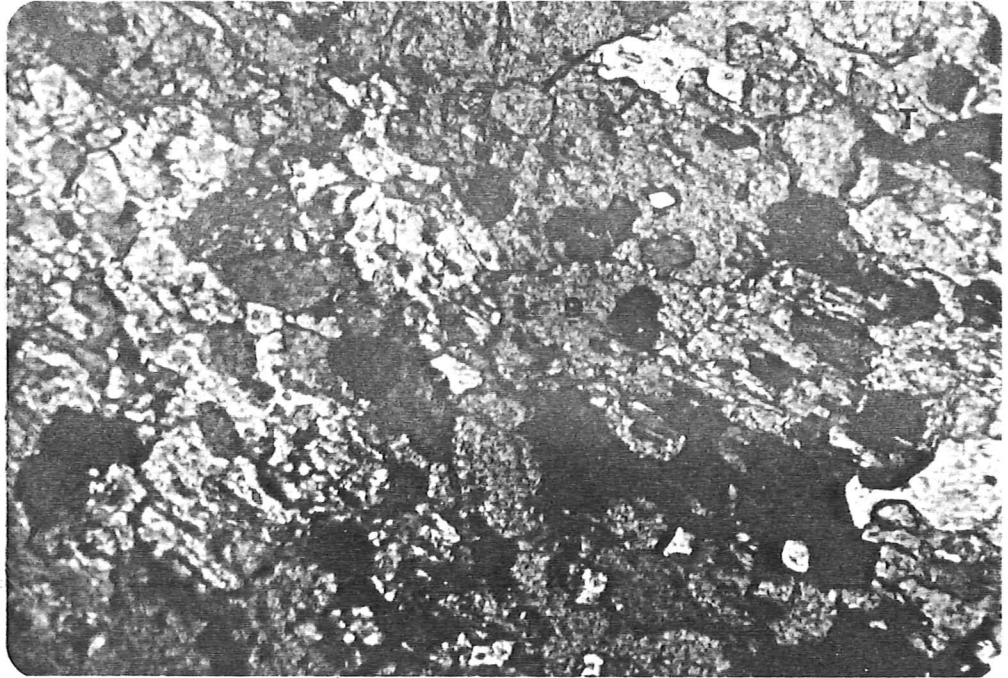
- A. Poikiloblastic diopside (D) with calcite and quartz inclusions, and tremolite overgrowths (T). Typical disequilibrium texture, for the retrograde reaction



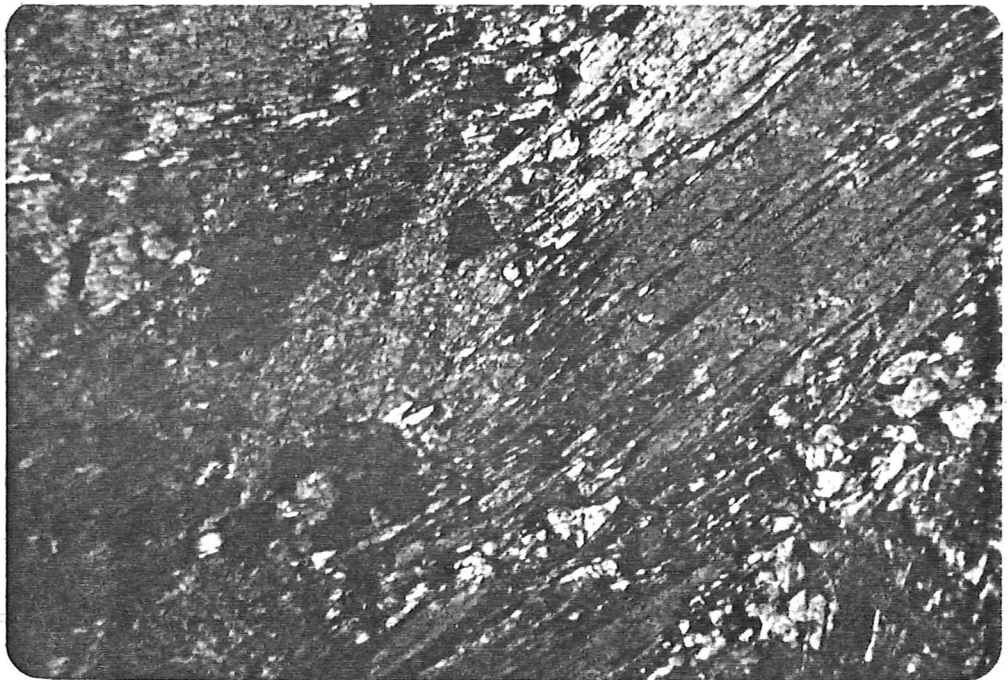
764-DR21.

- B. Ragged actinolite laths with interstitial xenoblastic calcite aggregates. Actinolitic horizons do not show a strong fabric. 764-LL12.

F.V. is 2mm across.



A



B

A distinction can be made between primary recrystallized calcite and calcite from retrograde reactions on the basis of texture. The primary calcites are large (2 mm) and twinned, showing a recrystallized polygonal texture. They are associated with porphyroblastic epidote and pyrite, which are elongate and parallel to the banding. The retrograde calcite is fine grained and xenoblastic and occurs as a reaction product along with tremolite (Plate 2b).

Interbedded with the calc silicates are quartz-feldspar-mica horizons which predominate towards the top of the Bimba Formation.

The preferred orientation of the micas defines the schistosity which is parallel to the compositional layering. The biotites are brown, varying in size from 0.1 - 2.0 mm, average ~1.0 mm. Primary muscovite is less abundant but forms long thin needles up to 5 mm in length.

Quartz and feldspar are fine grained, average ~0.2 mm and texturally could be called a microgneiss, with feldspar more abundant than quartz. Both minerals show a recrystallized fine grained polygonal texture. However, large relict dusty quartz and feldspar grains occur interstitially. Large undulose quartz grains show subgrain development and serrate grain boundaries. Relict feldspars may be partially sericitized, zoned and twinned, indicating metamorphic disequilibrium.

4.4 Original Rock Types

The lowest stratigraphic association, feldspar-hornblende-epidote-actinolite is equivalent to a metamorphosed amphibolite (Hyndman, 1972) and may have formed in two ways:

- (1) from a basaltic tuff or tuff contaminated by carbonate;
- (2) shaley limestone or calcareous shale.

If the association is interlayered with calcareous metasediments, then it is more likely to be the second alternative. The amphibolite here is underlain by an albite rich unit, possibly derived from a volcanic source (Gabell, 1978), and overlain by calc silicates, derived from sediments. Sodium metasomatism (Wiltshire, 1975) has also been proposed for the formation of the albite rich units. Just as the origin of the albites is enigmatic, so is the origin of the "amphibolite," since it is sandwiched between the two alternatives. A mixture of the two origins is a third alternative.

The calc silicate mineralogies are typical of metamorphosed marls and

siliceous dolomitic limestones (Winkler, 1979). Minerals typical of iron rich marls are epidote-actinolite \pm quartz and those of limestones are tremolite-calcite-diopside and quartz. The iron content is probably the most important factor in deciding which minerals will form.

The CaO/Na₂O ratio (Appendix IV) is high for the calc silicates, indicating that the calcium has been derived from carbonates rather than feldspar (Senior and Leake, 1977), which is what one expects from these carbonate rich calc silicates,

The Mixed Horizon consists of interbedded pelites with marls and impure limestones. A high iron content is suggested by the presence of siderite as well as calcite.

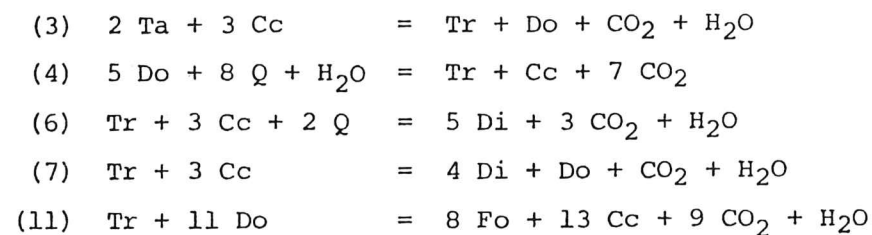
The upper stratigraphic units consist of quartz-feldspar-mica \pm Sillimanite, which is typical of metamorphosed pelites or greywackes (Winkler, 1979). As the SiO₂ value decreases the Al₂O₃, Na₂O and K₂O values increase. This trend in pelites reflects the increase in clay components as the detrital quartz content decreases (Fig. 4).

4.5 Pressure-Temperature Conditions

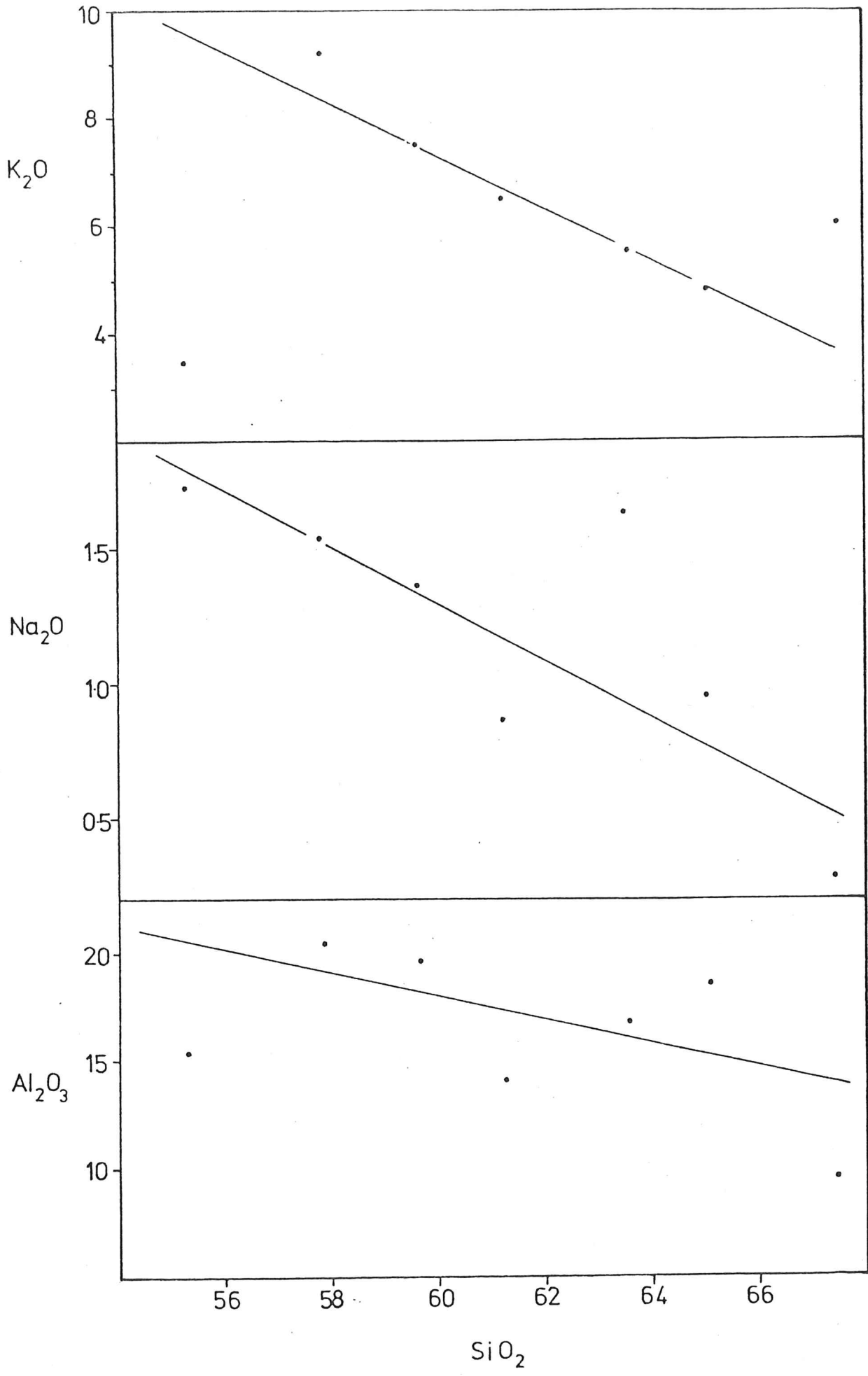
There are few diagnostic mineral assemblages in the calc silicates that can accurately define P-T conditions. The overlap of high grade and low grade minerals, due to disequilibrium, compounds the problem of defining P-T conditions.

The presence of high grade minerals such as diopside, andradite, scapolite and hornblende, suggest temperatures $>500^{\circ}\text{C}$. The steepness and lack of crosscutting tie lines make pressure estimations impossible.

In the calc silicates the absence of talc and wollastonite, suggest high values of X CO₂ (Winkler, 1979). At high X CO₂, tremolite forms instead of talc. Tremolite-calcite and tremolite-calcite-diopside-quartz are two common mineral associations. These are defined by five isograds on the T-X CO₂ graph (Fig. 5).

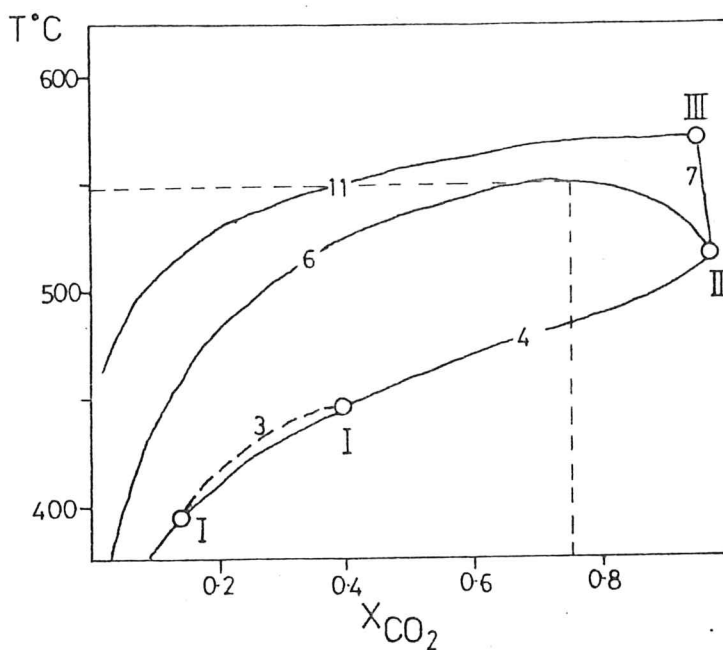


PELITIC TRENDS
 Al_2O_3 , Na_2O , K_2O vs SiO_2 fig 4

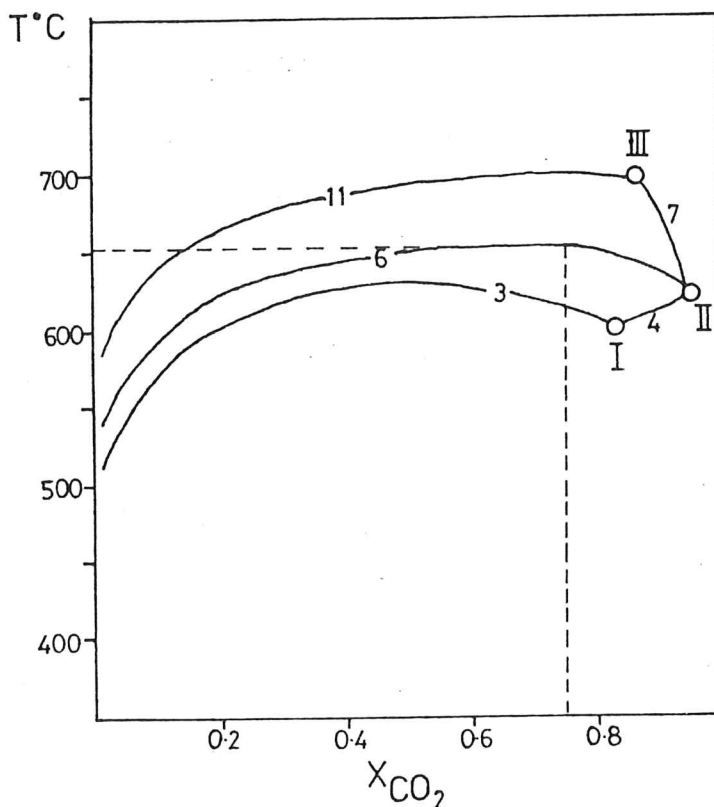


$T - X_{\text{CO}_2}$ at 2kb, 5kb

fig. 5



2 kb
(Skippen 1974)



5 kb
(Winkler 1974)

The shaded area shows where the tremolite-calcite and tremolite-calcite-dio-
 pside-quartz associations are stable. This is defined by 5 isograds:

- | | |
|--|--|
| (3) 2 Talc + 3 Calcite | = Tremolite + Dolomite + CO ₂ + H ₂ O |
| (4) 8 Quartz + 5 Dolomite + H ₂ O | = Tremolite + 3 Calcite + 7 CO ₂ |
| (6) Tremolite + 3 Calcite + 2 Quartz | = 5 Diopside + 3 CO ₂ + H ₂ O |
| (7) Tremolite + 3 Calcite | = 4 Diopside + Dolomite + CO ₂ + H ₂ O |
| (11) Tremolite + 11 Dolomite | = 8 Forsterite + 13 Calcite + 9 CO ₂ |

Minerals that coexist at the invariant points, I Tr-Tc-Cc-Do-Q
 II Do-Q-Di-Cc-Tr
 III Fo-Di-Tr-Do-Cc

The absence of talc, forsterite and dolomite define the shaded area, within which the two associations occur. Reaction (6) is the most important since it defines the relationship between tremolite, calcite and diopside. Both sides of the isograd need to be taken into consideration as a result.

Since the pressure cannot be determined here, the temperatures (Fig. 5) are shown for various pressure conditions, which relate to the five isograds (Skippen, 1974).

Hyndman (1972) suggests that values of $X_{CO_2} < 0.25$ are unlikely for metamorphosed limestones. This value has been used as the lower limit for X_{CO_2} .

Wiltshire (1975) was able to calculate P-T conditions for the metamorphisms. He proposed pressure-temperature conditions of 4-6 kb and 500-650°C for M1 and M2, and a pressure of ~4 kb and temperature of ~400°C for M3.

5. MINERALIZATION

5.1 Introduction

The mineralization is stratiform and stratabound showing a strong concordance with the compositional layering of the Bima Formation. This layering in the sulphide horizons may have occurred in three ways:

- (1) it is original sedimentary layering (syngenetic);
- (2) it is a result of metamorphism, metamorphic layering;
- (3) has occurred as a selective replacement of a stratigraphic horizon by metal bearing solutions.

The sulphide horizons have been metamorphosed, which poses a problem in identifying the original texture and genesis of the mineralization. McDonald (1967) and Vokes (1969) both stress that sulphides recrystallize very easily during metamorphism, so that the final texture may bear no resemblance to the original one.

5.2 Mineral types

The most abundant mineral is pyrite, forming more than 90% of the mineralization. It is accompanied by varying amounts of pyrrhotite, sphalerite, chalcopyrite and haematite-magnetite.

The following minerals were identified in polished and polished thin sections are listed in decreasing order of abundance:

1.	Pyrite	FeS_2
2.	Melnikovite Pyrite	FeS_2
3.	Chalcopyrite	CuFeS_2
4.	Sphalerite	ZnS
5.	Pyrrhotite	Fe_{1-x}S
6.	Magnetite-haematite	$\text{Fe}_3\text{O}_4\text{-Fe}_2\text{O}_3$
7.	Marcasite	FeS_2
8.	Goethite	$\text{FeO}\cdot\text{OH}$
9.	Covellite	CuS
10.	Arsenopyrite	FeAsS
11.	Ilmenite	FeTiO_3
12.	Native Copper	Cu

Noticeably absent are lead minerals, especially galena. Pyrite is the dominant mineral and shows the greatest variety of textural fabrics.

5.3 Textures

The mineralization occurs as both massive horizons and as disseminated grains. They are hosted, predominantly by the calc silicates from the Mixed Horizon, especially the carbonates.

The pyrite horizons are banded like their metamorphosed host. This type of mineral banding is common in regionally metamorphosed terrains and is probably one feature of the fabric which survives metamorphism (Vokes, 1969). Smaller lenses and stringers are flattened and parallel to the fabric also.

Pyrite porphyroblasts, up to 4 mm, have developed as a result of metamorphism. Most are clean, but many contain calc silicate inclusions, indicating growth in situ.

These massive horizons frequently show annealed textures with the pyrites forming triple point junctions. Chalcopyrite may migrate to these junctions (Plate 3a) or along the pyrite grain boundaries because of its greater mobility (Lawrence, 1973). In contrast to this, idiomorphic pyrites develop as disseminated grains, where they are able to attain their minimum free energy state (Stanton, 1964). These are fine grained, average ~1 mm.

Brecciated pyrite is a distinctive texture (Plate 3b) which indicates brittle failure. The shattered pieces vary in size but maintain curvilinear grain boundaries. It would appear that the grains prior to brecciation were large (porphyroblastic). This suggests that the porphyroblastic development was associated with the earlier metamorphic events M1 or M2, whilst brecciation is a late event probably associated with the last structural deformation and M3.

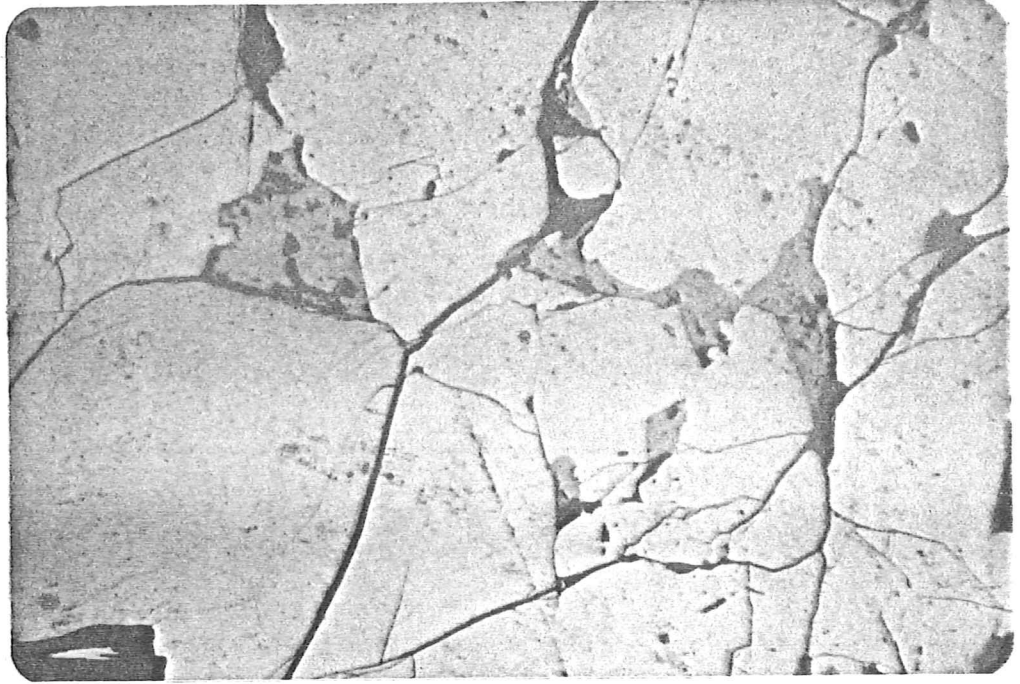
A large proportion of the pyrite has altered to melnikovite pyrite, a textural form of pyrite (Plate 3c). This alteration changes from an initial dusty appearance to the typical colloform texture. Melnikovite pyrite is found in low temperature retrograde environments (R. Both, pers. comm.). Often the melnikovite-pyrite shows a skeletal fabric which may be a precursor to the development of boxwork fabric. Marcasite frequently occurs with the melnikovite, suggesting that it too is a low temperature replacement of pyrite. It forms a myrmekitic or graphic texture of veinlets (Plate 4a).

Secondary pyrite veinlets occur interstitial to the host grains or along the cleavage planes of minerals such as amphibole, epidote and diopside. These have seemingly been mobilized in solution from the massive pyrite horizons.

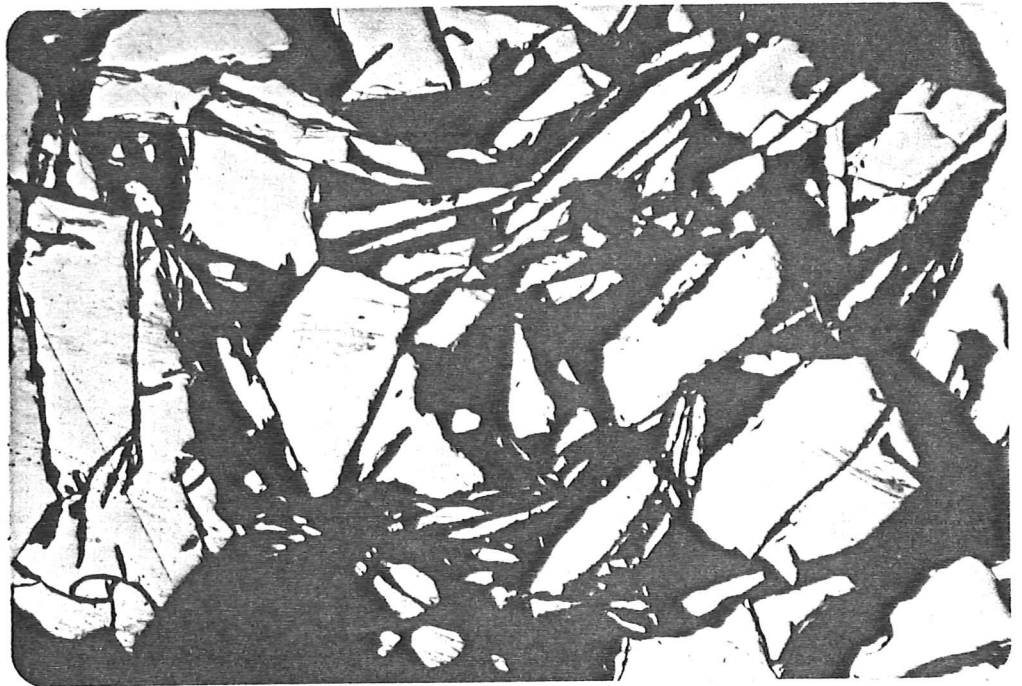
PLATE 3

- A. Massive pyrite horizon, showing partial triple point junction development due to recrystallization. Chalcopyrite aggregates at these junctions and along grain boundaries, because of its greater mobility. Minor fracturing in pyrite is observed. 764-LL10.
- B. Brecciated texture in pyrite due to brittle failure. Fragments are elongate, probably breaking along crystallographic orientations. 764-LL6.
- C. Melnikovite pyrite appears as a dusty haze overlying the pyrite. This is a low T°, retrograde alteration product of pyrite. 764-68(MP4).

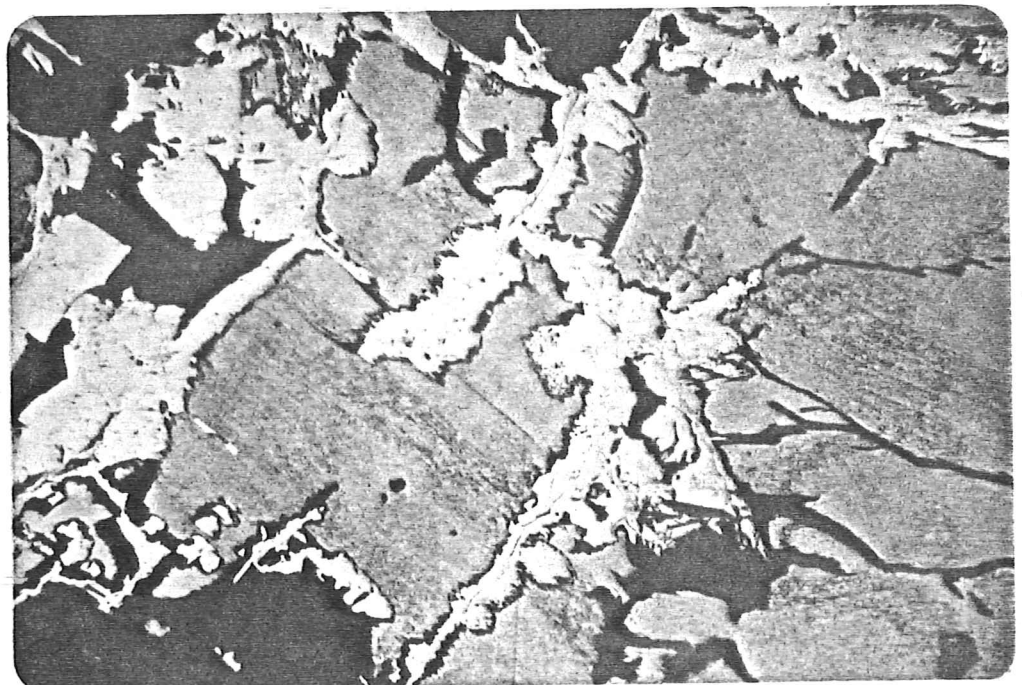
F.V. is 2mm across.



A



B



C

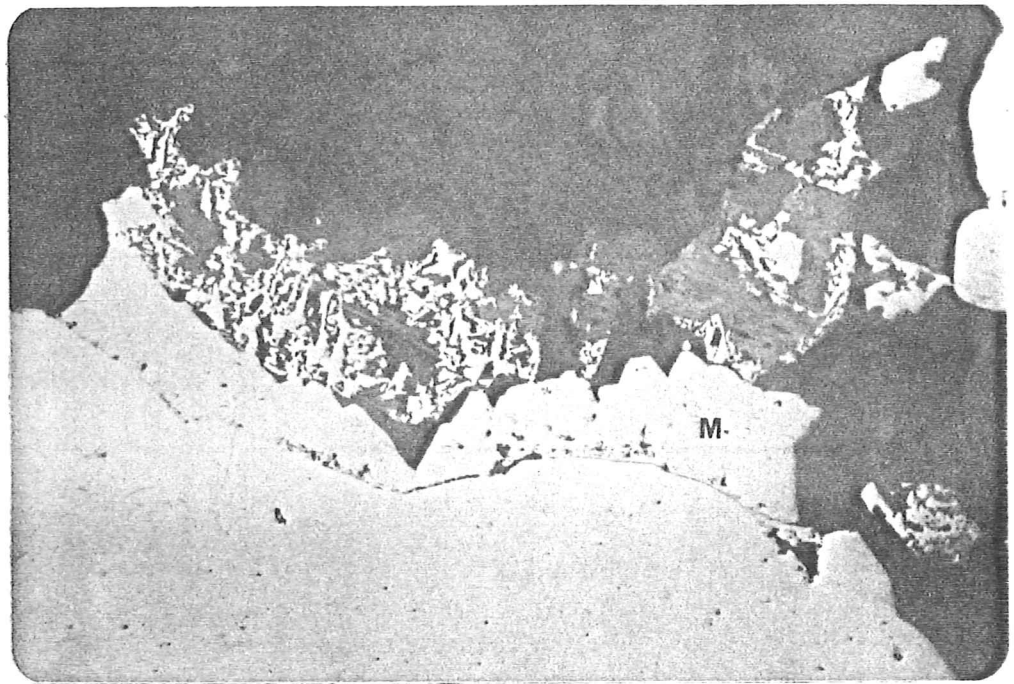
PLATE 4

A. Marcasite (M) overgrowth on pyrite, showing a graphic or myrmekitic texture with the metamorphic host. Marcasite is a low T, alteration product of pyrite. 764-DR9.

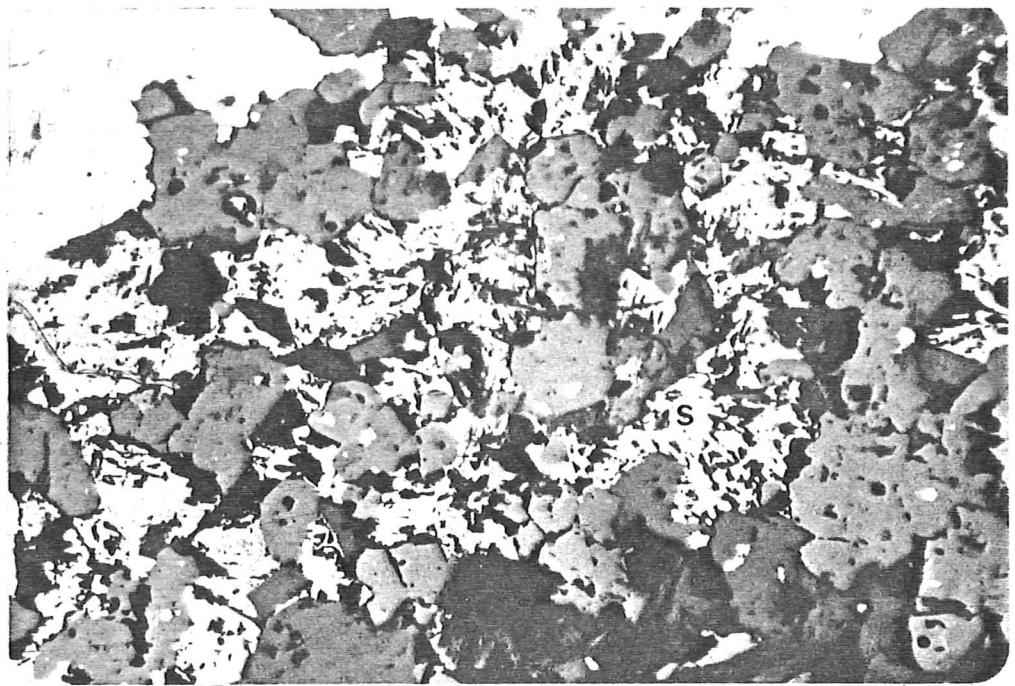
B. Sphalerite (S) showing poor development of crystal faces because of its low form energy. It occurs here as irregular interstitial aggregates. 764-CR10.

C. Brecciated pyrite and covellite. Covellite, a supergene alteration product has completely replaced chalcopyrite. 764-LL6.

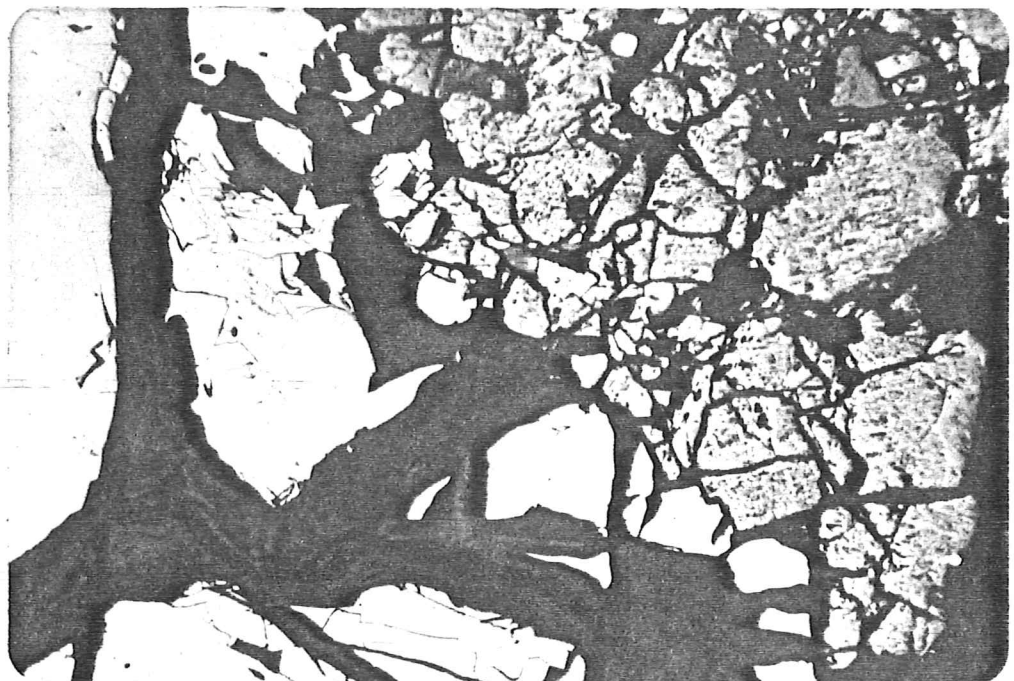
F.V. is 2mm across.



A



B



C

The pyrite frequently shows a caries texture (Schwartz, 1951) with the enclosing metamorphic minerals, indicating its low form energy (Stanton, 1964).

(Scott, 1974),

Most of the pyrrhotite is hexagonal, the high temperature form, however some low temperature equilibration has occurred since monoclinic rims can be found surrounding these. Pyrrhotite occurs mostly as ovoid inclusions in the pyrite along with chalcopyrite. A common metamorphic reaction with increasing grade is the alteration of pyrite \rightarrow pyrrhotite (Vokes, 1969; McDonald, 1967), but this has not developed here.

Sphalerite and magnetite both exhibit a granule texture (Schwartz, 1951). This is typical of metamorphosed ore minerals that have low form energy and do not develop crystal faces (Plate 4b). The aggregates may be quite large, up to 2 mm, but the individual granules are small.

Magnetite commonly shows haematite alteration along its cleavage directions, thus appearing as a triangular network of lamellae.

Covellite occurs as a vivid blue supergene alteration of chalcopyrite (Plate 4c). Where the chalcopyrite has not been completely replaced it occurs as relict cores rimmed by the covellite. Large chalcopyrite grains, ~2 mm, develop where it occurs in greatest abundance, but mostly it forms inclusions in the pyrite.

5.4 Occurrence

All the mineralization in the Bimba Formation is stratiform and most is hosted by the calc silicates of the Mixed Horizon. Chemical sedimentation of the carbonates may have been a controlling factor in mineralization.

Pyrite is associated with the calc silicates, with pyrite-calcite and pyrite-epidote being the most common associations. These pyritic calc silicate horizons are coarser grained than the interbedded quartz-feldspar-mica, which may be due to the ease of recrystallization and development of porphyroblasts of the calc silicates.

The calcite-pyrite association is coarse grained with pyrite porphyroblasts up to 4 mm and recrystallized calcite up to 2 mm developed. Where the pyrite is massive, then polygonal textures occur.

Elsewhere, pyrite has an intimate association with epidote, occurring as coarse grains or bands with the epidote, or as a skeletal texture interstitial

to it. Where pyrite is less abundant it occurs as fine grained idiomorphic cubes within the epidote aggregates.

Pyrite occurrence in the quartz-feldspar-mica horizons is limited to biotite rich horizons.

Sphalerite, pyrrhotite and chalcopyrite are all associated with the pyritic-calc silicate horizons and probably form part of the same mineralization.

The iron oxides, magnetite-haematite, are scarce in the Bimba Formation, but occur in greater abundance below it. This transition from an iron oxide to an iron sulphide facies suggests a change from an oxidizing to a reducing environment as we pass into the Bimba Formation.

5.5 Trace Elements in Pyrite

A trace element study of the pyrites was undertaken in order to determine any possible genetic indicators (Appendix II). Cobalt (Co), Nickel (Ni) and the cobalt:nickel ratio in pyrites has long been regarded as a good genetic indicator (Juve, 1968; Mookherjee and Philip, 1979; Cambel and Jarkousky, 1966). The following values for Co:Ni have been used as genetic indicators:

Sedimentary pyrite	Co:Ni	<1	(Loftus-Hills and Solomon, 1967)
Hydrothermal pyrite	Co:Ni	>1	(" " " ")
Volcanogenic pyrite	Co:Ni	>1	(Plimer, 1977)
Volcanogenic pyrite	Co:Ni	>5	(Bralia, et al., 1979)

There is a problem with Co:Ni determinations in metamorphosed terrains. With increasing grade the reaction pyrite \rightarrow pyrrhotite is regarded as common (Bralia, et al., 1979), and with this change the nickel is preferentially concentrated in the pyrrhotite, whilst the cobalt remains in the pyrite. This causes an increase in the Co:Ni ratio of pyrites from metamorphosed terrains. However, the lack of pyrrhotite in the Bimba Formation, suggests that the metamorphic influence on the Co:Ni ratio has been minimal, and the values obtained may be real genetic indicators.

The Co:Ni ratios (Table 1) obtained from the pyrites show a wide range of values from 0.069-38.0. The average value is 5.2 and most ratios are >1. The range for cobalt is 2-1710 ppm, average 330 and for nickel 5-670 ppm, with an average of 110 ppm.

TABLE 1

TRACE ELEMENT CONTENT OF PYRITE (PPM)

Sample	Cu	Zn	Co	Ni	Co:Ni
764.LL1	40	760	2	29	.07
764.LL7	1160	55	30	60	.5
764.LL8	1230	20	670	44	15.22
764.CR4	205	45	20	39	.51
764.CR11	2150	440	630	670	.94
764.CR14	580	260	570	440	1.3
764.DR5	240	10	1710	45	38.0
764.DR8	70	7	23	10	2.3
764.DR9	70	10	20	14	1.43
764.DR10	40	10	14	5	2.8
764.36	6000	30	1000	135	7.4
764.65	455	6100	70	21	3.3
764.67	1970	1050	240	135	1.77
764.75	23	90	150	50	3.0
764.78	75	275	100	50	2.0
764.96	29	50	24	22	1.09
Average	896	576	330	110	5.16
Range	23-6000	7-6100	2-1710	5-670	.07-38.0

Values for massive sulphides of volcanogenic exhalative origin (Bralia, et al., 1979) are:

Cobalt	usually	>100 ppm,	average	486 ppm
Nickel	"	<100 ppm,	"	56 ppm
Co:Ni	"	5-50 ppm,	"	8.7 ppm

A comparison with this data, indicates that the pyrites here are of the same order. This alone is not conclusive that they may be volcanogenic exhalative in origin, however it is likely.

The textural evidence and the continuous stratiform nature of the sulphides suggests that they are syngenetic in origin, either sedimentary or volcanogenic.

Also in the pyrites (Table 1) are significant concentrations of copper, 23-6000 ppm, and zinc, 7-6100 ppm. The other trace elements are either low or below the limit of detection (Appendix II). These are not valuable genetic indicators.

6. TRACE ELEMENT GEOCHEMISTRY OF MP1-MP10

Data on the trace element geochemistry of ten drill holes at Meningie Well (MP1-MP10) was available from Esso Australia. Of particular interest were the Cu, Pb, Zn, Co, Ni, Mn, Ba and W values. Abundance vs. Depth graphs for Cu, Pb, Zn, Co (Fig. 6) were correlated with the stratigraphy, from which several trends could be observed.

6.1 Element-Element Relationships

From the graphs (Figure 6) it can be seen that the distributions of the four elements Cu, Pb, Zn and Co are quite different. On close inspection a few trends emerged.

The strongest correlation is that between copper and cobalt whose peaks are sympathetic. These peaks are usually associated with the massive pyrite horizons. The copper probably occurs mostly as chalcopyrite, whilst the cobalt is accommodated in the pyrite. Elsewhere in the Willyama Complex cobaltian pyrite has been recognised (Plimer, 1977).

A crude relationship between lead and zinc exists, with zinc values mimicking the lead. Pb values are generally low throughout, making correlations difficult. Zinc on the other hand, shows high concentrations and greater variability. This produces erratic peaks, some of which mimic the Cu-Co-pyrite, but elsewhere are completely independent of element patterns.



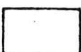


Zinc and copper are almost mutually exclusive, with high zinc values where copper values are low, and vice versa. An overlap of these two extremes does occur.

Manganese and barium have similar trends. They occur in greater abundance in the mineralized horizons than elsewhere, but do not show distinctive relationships with the four main elements.

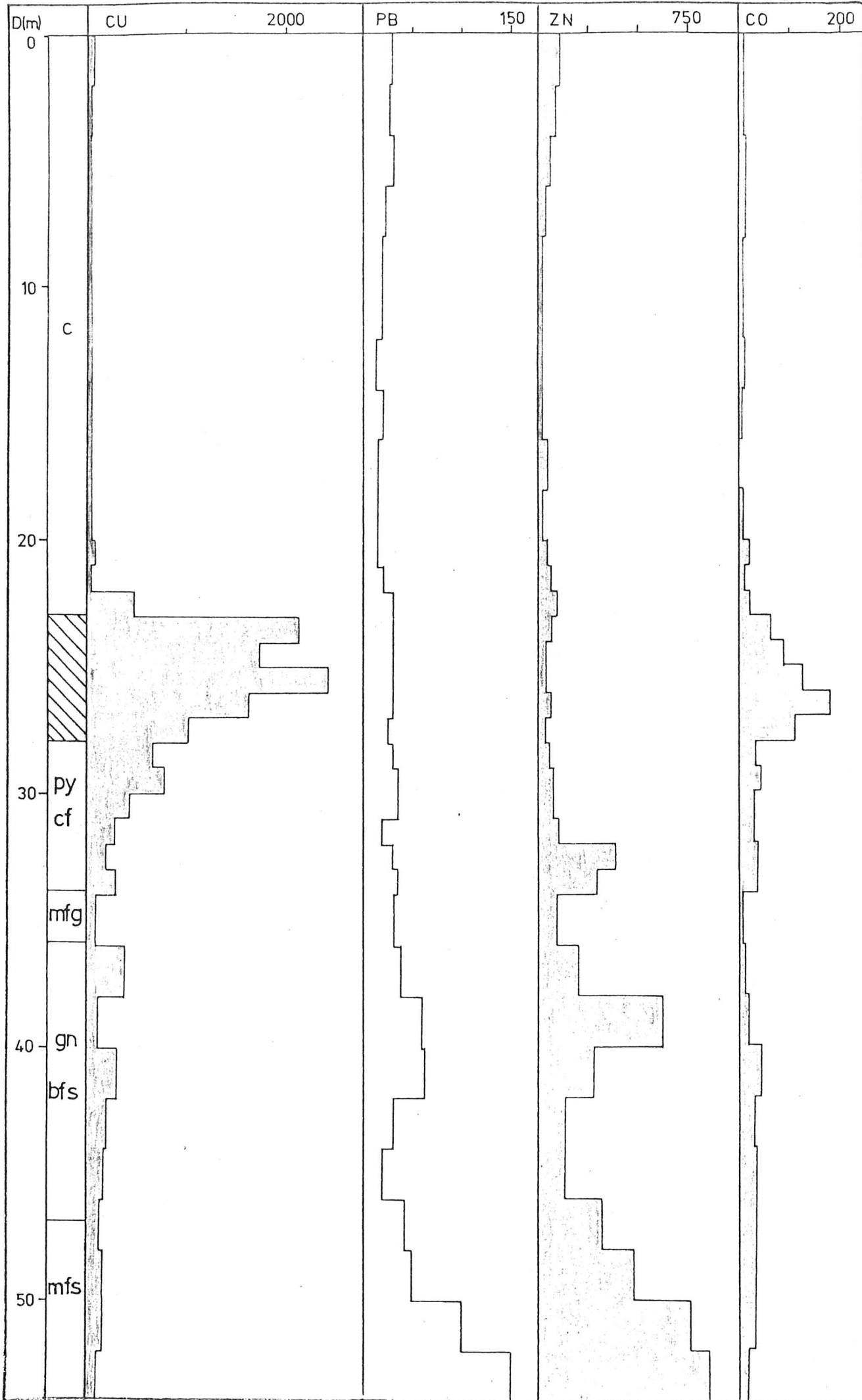
6.2 Trace Elements and Stratigraphy

High copper values occur in two types of host. Firstly, in the massive pyritic horizons along with the calc silicates and secondly, in the mica schists/microgneisses which are interbedded throughout the Bimba Formation. The values for Cu are variable with most greater than the average in sedimentary rocks (Table 2). This suggests that it is necessary to propose either a mechanism for concentrating the Cu, or an independant source for the Cu.

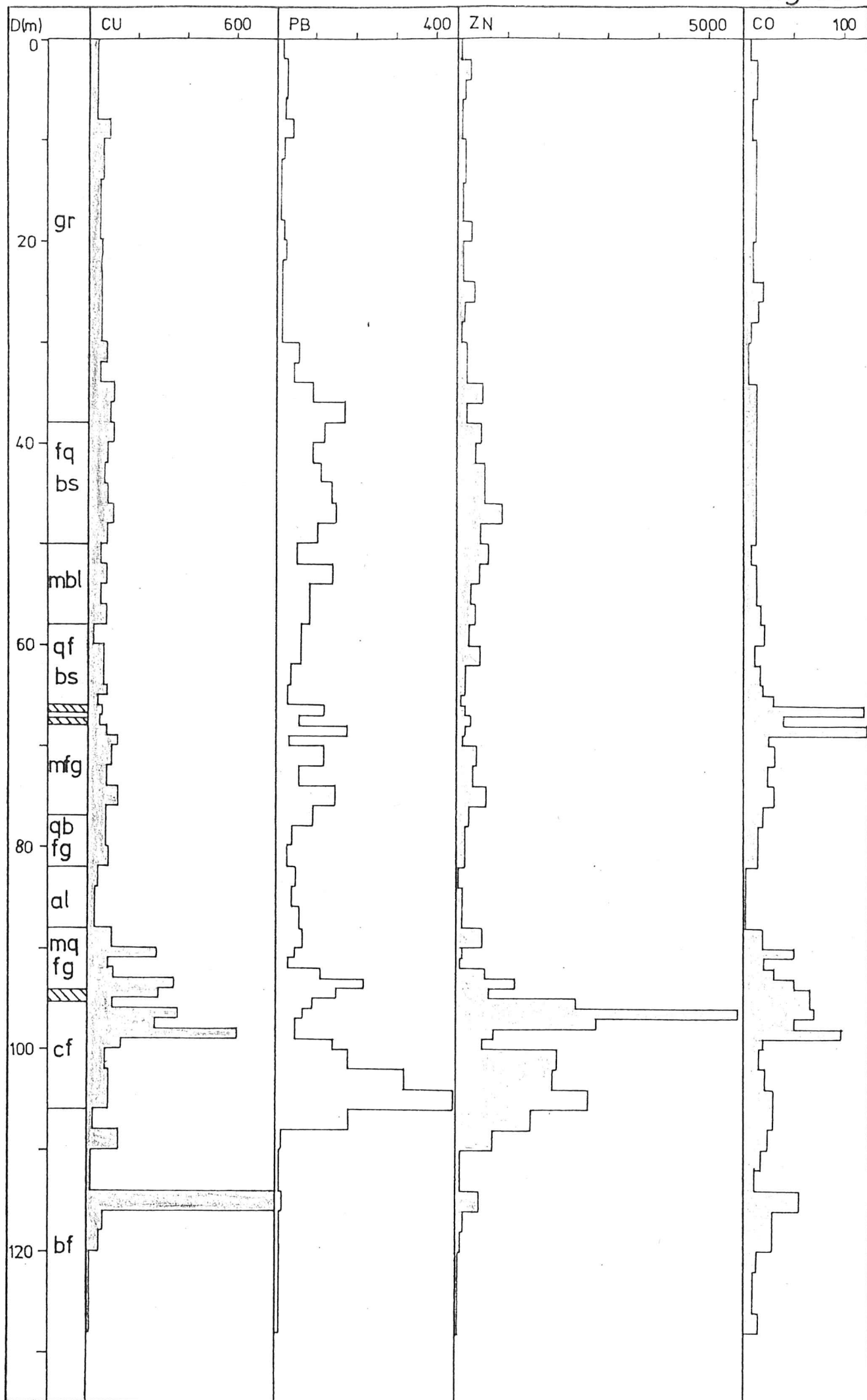
DEPTH vs ABUNDANCE GRAPHS, MP1 - MP10

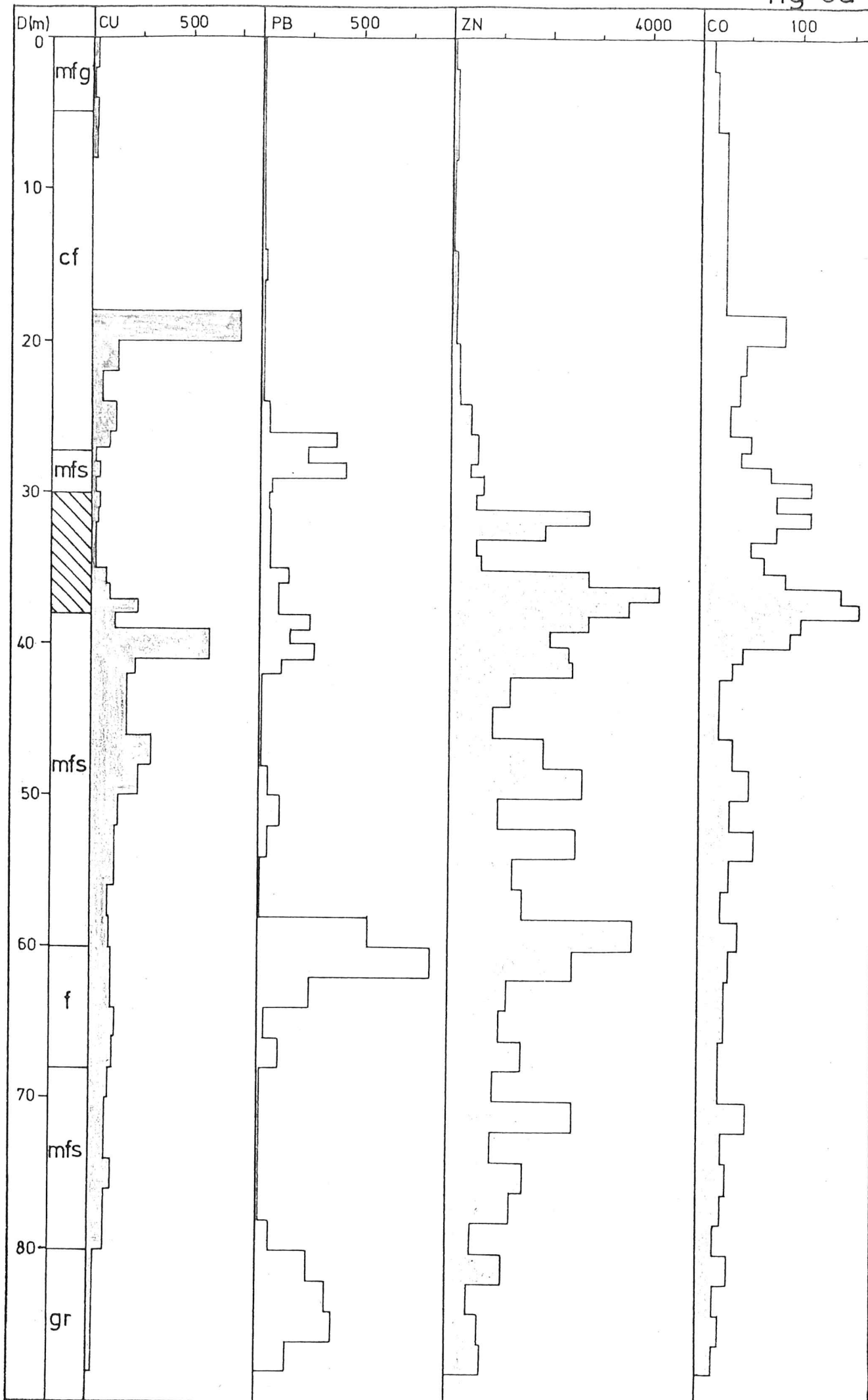
c	calc silicate
f	feldspar
py	pyrite
m	mica
g	gneiss
b	biotite
s	schist
mbl	marble
gt	garnet
q	quartz
gr	graphitic
al	alaskite - pegmatite
ch	cherty
	Sulphide Horizon
	Cu values (ppm)
	Pb values (ppm)
	Zn values (ppm)
	Co values (ppm)
D(m)	Depth in metres

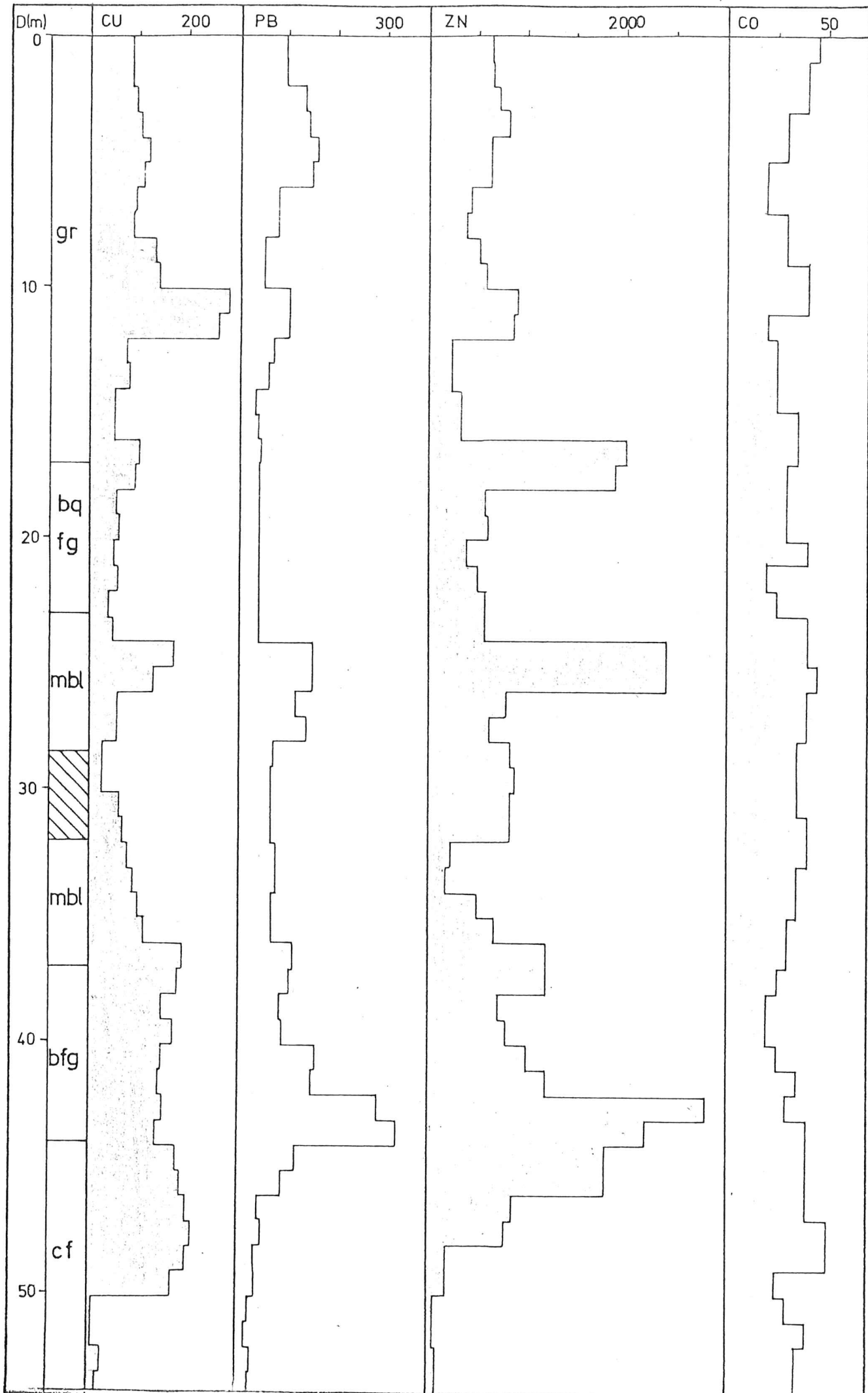
MP2 & MP9 missing because incomplete analyses

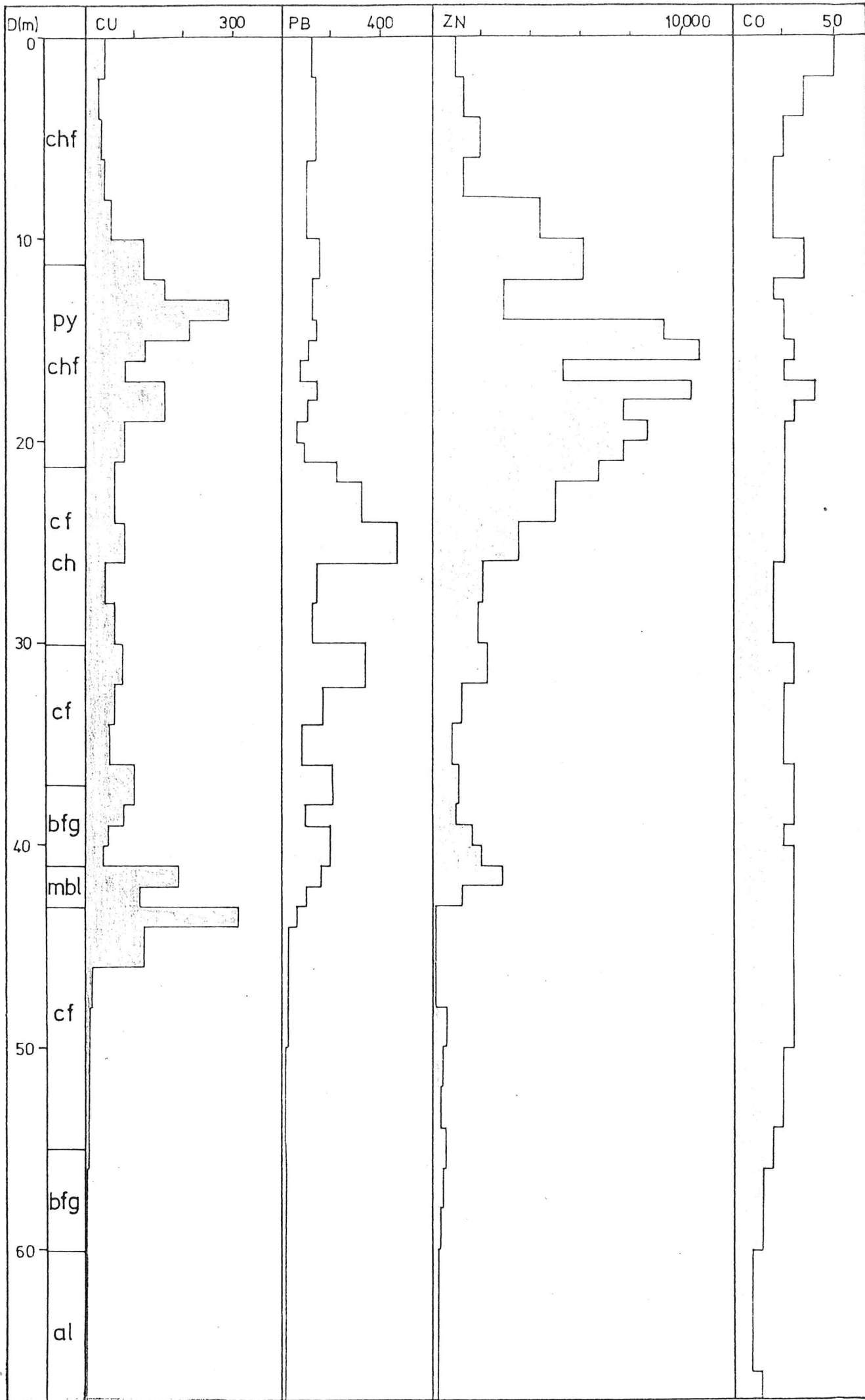


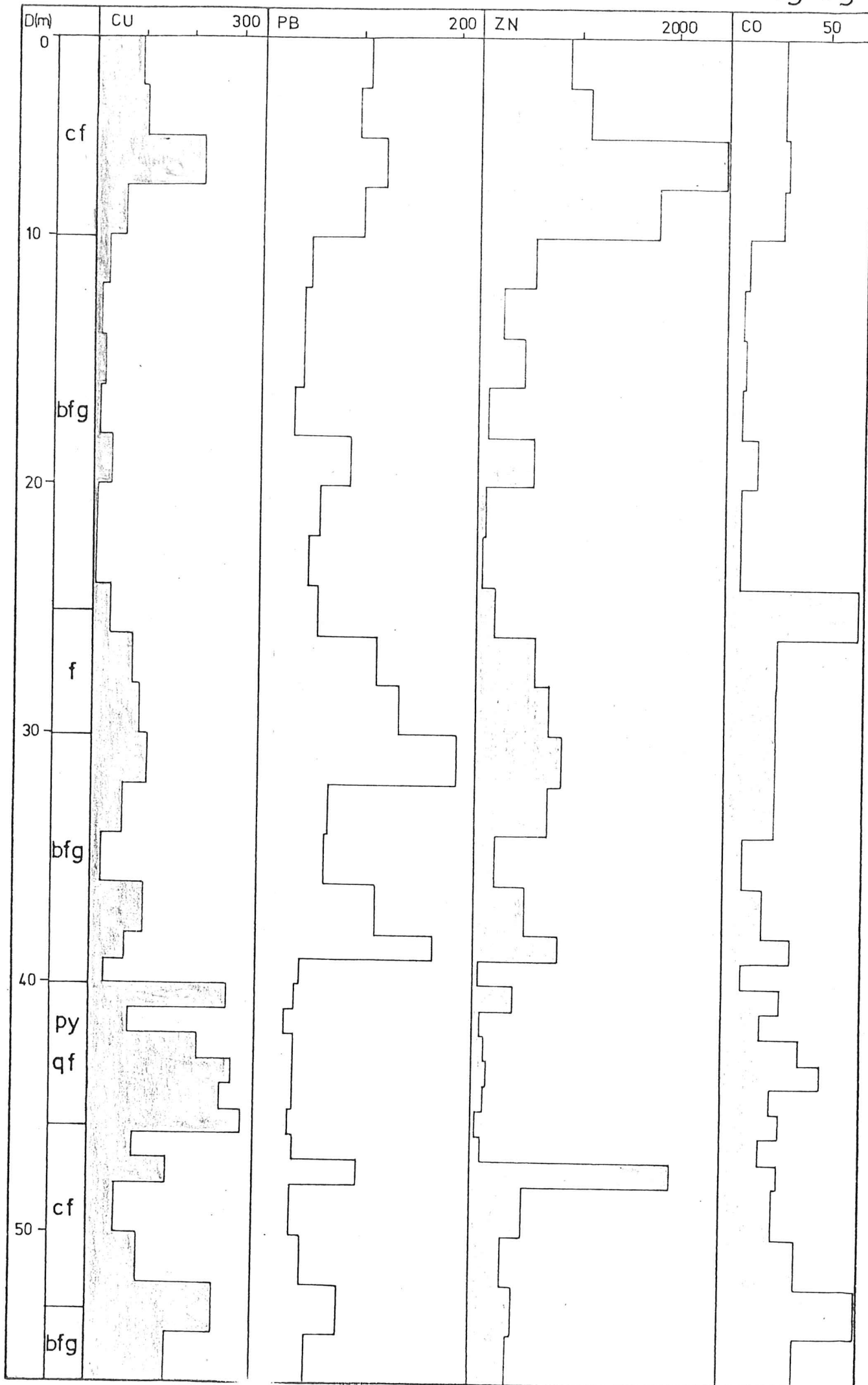












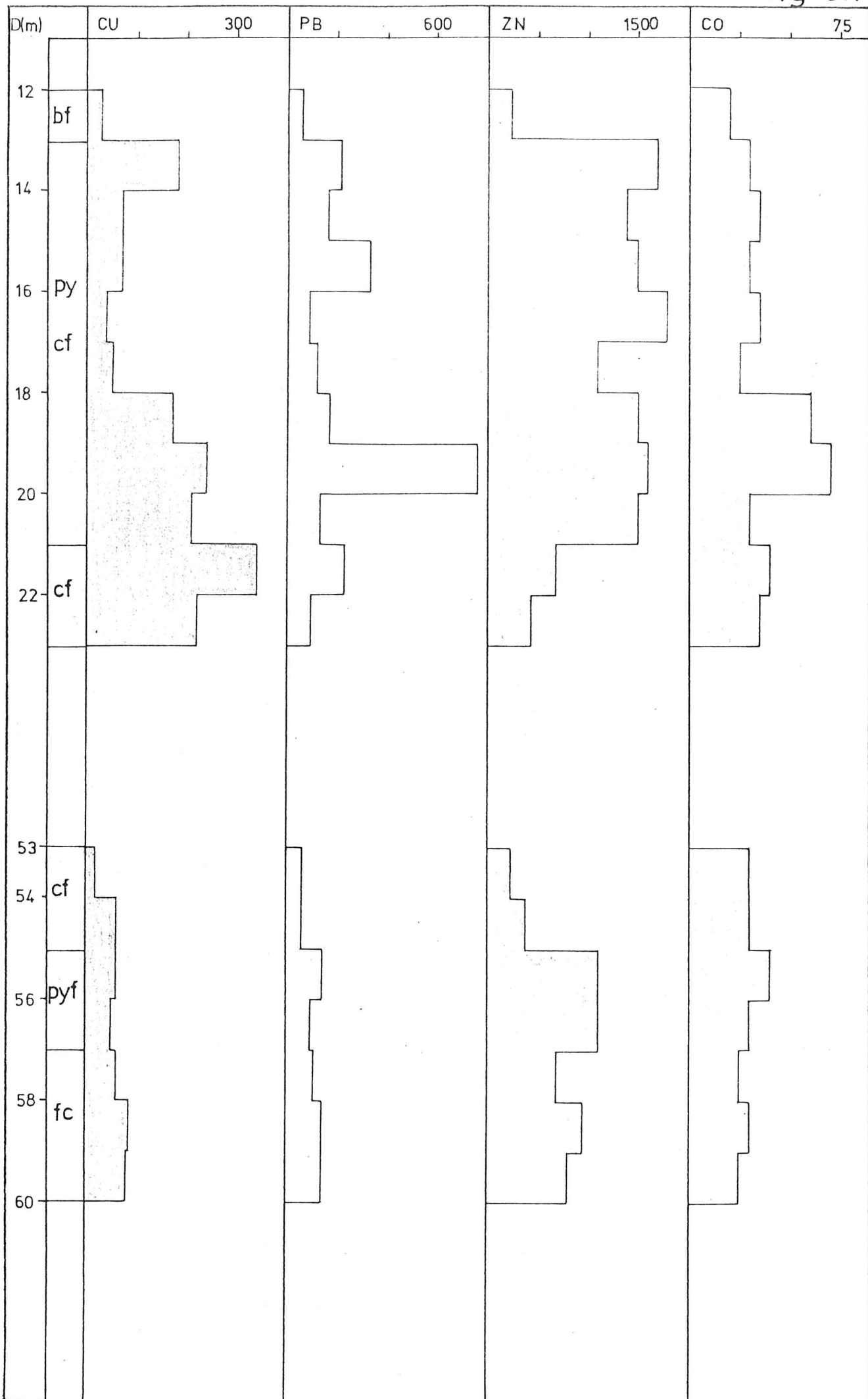


TABLE 2 AVERAGE TRACE ELEMENT CONTENT OF IGNEOUS AND SEDIMENTARY ROCKS

	IGNEOUS			SEDIMENTARY			
	U/mafic	Mafic	Felsic	Lmst	SSt	Shale	Bl.shale
Cu	80	140	30	5-20	10-40	30-150	20-300
Pb		±412	48	5-10	10-40	20	20-400
Zn	50	130	60	4-20	5-20	50-300	100-1000
Co	200	45	5	0.5-2	1-10	10-50	5-50
Mn	1300	2200	600	1300	385		
Ni	1200	160	8	3-10	2-10	20-100	20-300
Ba	15	270	830	20-200	100-500	300-600	450-700
W		Av. 2		1.8	1.6		

From "Geochemistry in Mineral Exploration"
by H.E. Hawkes and J.S. Webb.

Lead has low values in the main pyritic horizon, suggesting that its concentration is not related to pyrite mineralization. Lead values are highest in the schists (QFM), extending into the graphitic horizon. Even though Pb values are low, they show enough variability to frequently extend beyond the average sedimentary concentration. These larger values are either due to a concentrating mechanism, maybe a greater abundance of mica or feldspar with Pb incorporated, or due to an independent source. Low Pb values in the calc silicate horizons correlates with low averages in limestones.

Even though the values for zinc are high, sphalerite was scarce. Zinc shows very sharp, erratic peaks which occur randomly throughout the Bimba Formation, indicating no stratigraphic control. The maximum values are much higher than average sedimentary contents, making it necessary to introduce an independent, possibly erratic, source, or a concentrating mechanism.

The occurrence of cobalt is related to that of copper and the main pyritic horizons. Cobalt mimics impeccably even very thin pyritic horizons (Fig. 6c). The correlations between Cu-Co-pyrite is strong, and stratigraphically occurs in the calc silicates of the Mixed Horizon.

Barium values are high throughout the area. These are not associated with any particular stratigraphic horizon. Barium values here are much higher than average sedimentary contents, but since barium is very mobile under metamorphic conditions, this may have concentrated the values.

Similarly, manganese values are high in all stratigraphic horizons, mimicking barium values. The manganese values are slightly higher than average limestones. Where it does concentrate, it usually occurs over a short interval, suggesting a lower clastic component over that interval.

Tungsten values are low, below the detection limit, which is typical of sedimentary sequences.

The trace elements from the whole rock data (Appendix IV) indicate the same trends as the geochemistry from the MP wells.

6.3 Trace Elements and Lateral Variation

Lateral variation of the trace elements occurs. This can be seen by comparing the ranges of values for the trace elements in the individual drill holes (Fig. 2 - back pocket). This variation is supported by gossan analyses (Esso). Distinct domains occur, e.g. MP1, MP2, MP3 which are stratigraphically overturned, are Cu rich, both in geochemistry and gossan analyses. This contrasts with a Zn rich horizon (both gossan and geochemistry), in MP4, MP6, MP7 which are stratigraphically the right way up. This suggests that the two domains are on the opposite limbs of a fold.

This folding, is probably isoclinal, associated with the earliest regional deformation (Wiltshire, 1975). The lateral changes in trace elements appear to be rapid, but if we take into consideration this folding, then the unfolded facies variation would not be quite as sharp.

Thus two distinct domains, a copper rich and zinc rich one, can be distinguished. The copper domains are predominantly associated with the pyritic calc silicates, where the zinc values are low. Zinc domains tend to be a little more erratic, but maxima occur in the pyritic horizons, suggesting that pyrite formation was ubiquitous with the domains superimposed on it. Low lead values in cupriferous deposits (Mercer, 1976) is consistent with this two domain idea.

7. SUMMARY AND CONCLUSIONS

The basemetal mineralization in the Olary Province is hosted by a calc silicate horizon, the Bimba Formation. This horizon is defined between an albite rich unit and a graphitic metasiltstone. The Bimba Formation, itself can be subdivided into three sub units:

- (1) Calc Silicate Horizon, which is the result of chemical sedimentation of impure carbonates, with a possible volcanogenic influence.
- (2) Mixed Horizon, this consists of calc silicates which are interbedded with quartz-feldspar-mica layers, suggesting the addition of clastic sedimentation, possibly volcanogenic in origin, to the shelf type carbonate sedimentation.
- (3) Quartz-Feldspar-Mica Horizon, derived from clastic sedimentation.

Anomalously high MnO values in many calc silicates suggests that clastic contribution was low, but solution activity was high. Thus there is a trend for the chemical sediments of the impure, iron rich carbonates to gradually grade into the clastic sediments. This suggests a change from a shelf type carbonate environment to a more basinal sequence, indicating a deepening of the basin. The very fine grained graphitic siltstone overlying the clastics, is consistent with deepwater, fine grained clastic sedimentation.

A change of environmental conditions is also observed as we pass into the Bimba Formation. Below are mainly iron oxides indicating an oxidizing environment, which changes into a reducing one with mainly iron sulphide deposition in the calc silicates.

The banding in this stratigraphic horizon is sedimentary rather than metamorphic, for the following reasons:

- (1) Lack of homogenization of the trace element content of the various lithologies.
- (2) Diverse compositions in adjacent bands, indicating lack of homogenization.
- (3) High concentration of heavy accessories, which are frequently found concentrated in layers parallel to banding.
- (4) Gross lithological layering, schistosity and graphitic layering are all parallel. The graphitic layering must be sedimentary because of the inertness and immobility of graphite during metamorphism.

At least two metamorphic episodes can be recognised. Relict high grade minerals diopside, scapolite and andradite reflect an amphibolite facies metamorphism. These are overprinted by the retrograde reaction products tremolite, calcite and actinolite of the greenschist metamorphism. Mineralogical and textural disequilibrium is prevalent. The lack of indicator minerals and the disequilibrium make it difficult to determine pressure-temperature conditions. The lack of talc, suggests that X_{CO_2} was high. Using a value of $X_{CO_2} = 0.75$, the possible range of values are 550°C at 2 kb to 650° at 5 kb (Skippen, 1974).

Pyrite, the dominant sulphide, is stratiform with the sedimentary layering. This suggests that it is syngenetic. The pyrite textures indicate that they have suffered at least two stages of deformation, with the development of porphyroblasts and later, the brecciation of these porphyroblasts. Low temperature retrograde alteration to melnikovite pyrite and marcasite has also occurred.

Trace element contents (Cu, Pb, Zn, Co, Ni) are higher than average igneous and sedimentary rocks. This makes it necessary to invoke an additional source for these metals, e.g. volcanogenic exhalative. Lateral variation of the trace elements is evident by the occurrence of a Cu rich and Zn rich domain, superimposed on the pyrite mineralization. The Cu rich domains occur low in the stratigraphy associated with calc silicates, whilst the Zn domain tends to occur in the mixed horizons.

In summary, the mineralization, pyrite \pm chalcopyrite, \pm sphalerite, is probably volcanogenic exhalative because:

- (1) The Co:Ni ratios in pyrite are consistent with a volcanogenic origin.
- (2) Volcanic affinities in some calc silicates and in the albite rich horizons is probable.
- (3) Trace element contents are too high for ordinary sedimentary accumulation, making it necessary to suggest an additional source for the metals, e.g. volcanogenic exhalative.
- (4) The mineralization is stratiform and syngenetic, therefore it may be sedimentary with a volcanogenic-exhalative component.

Pyrite from a volcanogenic exhalative source is more common in shallower environments along with chemical sedimentation, whilst pyrrhotite forms in the deeper, basinal environments along with clastics, e.g. Broken Hill (Plimer and Finlow-Bates, 1978).

If a volcanogenic model is superimposed on the domains here, then the pyrite-Cu zone is typically proximal whilst the pyrite-Pb-Zn is distal, (Plimer, 1978). In contrast, Broken Hill which is a pyrrhotite-Pb-Zn association, would be favoured in a distal, deep water environment along with clastic sedimentation, if the volcanogenic exhalative model held true there also.

In conclusion, the environment for mineralization appears to have been controlled by the chemical sedimentation of the impure, Mn and Fe rich carbonates. There has been a gradual deepening of the basin, which can be seen by the change from an oxidizing to a reducing environment, and also by the change from the shelf type carbonate facies to the more basinal environment dominated by clastics.

ACKNOWLEDGEMENTS

This project was initiated by Rob Neile, Esso Australia (Minerals Division) Ltd. and supervised by Professor P. Ypma. Rob Neile was transferred early in the year and discussions were later held with Ian Herbison and Peter Robinson to whom I am most grateful.

Esso provided logistic support in the field and made available logs, samples from the MP wells, geochemical analyses and 1:10.000 maps of the area, without which the project would not have been possible. To them I am indebted.

I would like to thank my supervisor, Professor Ypma, whose guidance and final criticisms were appreciated. Thanks also to Dr. R.A. Both, for being available for help at all times.

A thank you is extended to the technical staff of the Geology Department whose help was appreciated in all stages of the project.

A very special thank you to all my fellow Honours Students, whose enthusiasm made the Honours Year a great experience.

* * *

BIBLIOGRAPHY

- Berry, R.F., Flint, R.B., Grady, A.E., 1978: Deformation of the Outalpa Area and its Application to the Olary Province, South Australia. *Trans. R. Soc. S.A.*, 102(2), 43-53.
- Bickle, M.J., and Powell, R., 1977: Calcite-Dolomite Geothermometry for Iron-Bearing Carbonates, The Glockner Area of the Tavern Window, Austria. *Contr. Mineral. Petrol.*, 59, 281-292.
- Bralia, A., Sabatini, G., Troja, F., 1979: A Revaluation of the Co/Ni Ratio in Pyrite as Geochemical Tool in Ore Genesis Problems, Evidences from Southern Tuscany Pyritic Deposits. *Mineral. Deposita*, 14, 353-374.
- Cambel, B., and Jarkovsky, J., 1966: The Possibility of Utilising of the Nickel and Cobalt in Pyrites as Indicators of Ore Genesis. *Geol. Sb.*, 17, 17-34.
- Campana, B., and King, D., 1958: Regional Geology and Mineral Reserves of the Olary Province. *Bull. Geol. Surv. S.A.*, 34, p. 134.
- Chatterjee, N.D., 1967: Experiments on the Phase Transition Calcite + Wollastonite + epidote = grossular - andradite_{SS} + CO₂ + H₂O. *Contr. Mineral. Petrol.*, 14, 114-122.
- *
Cobb, M.A., and Morris, B.J., 1970: The Weekeroo Amphibolite. *Unpub. Hons. Thesis, Univ. of Adelaide.*
- Deer, W.A., Howie, R.A., Zussman, J., 1966: *An Introduction to the Rock Forming Minerals.* Longman, London.
- Gabell, A.R., 1978: Geochemical and Structural Investigation of Willyama complex rocks, South Kalabity Station, South Australia. *Unpub. Hons. Thesis, Univ. of Adelaide.*
- Hyndman, D.W., 1972: *Petrology of Igneous and Metamorphic Rocks.* McGraw-Hill.
- Juve, G., 1974: Ore Mineralogy and Ore Types of the Stekenjokk Deposit, Central Scandinavian Caledonides, Sweden. *Sveriges Geol. Undersökning Yearbook 68*, 13, p. 162.
- Lawrence, L.J., 1973: Polymetamorphism of the Sulphide Ores of Broken Hill, N.S.W., Australia. *Mineral. Deposita*, 8, 211-236.
- Loftus-Hills, G., and Solomon, M., 1967: Cobalt, Nickel and Selenium in Sulphides as Indicators of Ore Genesis. *Mineral. Deposita*, 2, 228-242.

- Mawson, D., 1911: Chiestolites from Bimbowrie, South Australia.
Mem. Roy. Soc. S.A., 2.
- McDonald, J.A., 1967: Metamorphism and its Effects on Sulphide Assemblages.
Mineral. Deposita, 2, 200-220.
- Mercer, W., 1976: Minor Elements in Metal Deposits in Sedimentary Rocks -
A Review of Recent Literature. *Handbook of Stratabound and Stratiform
Ore Deposits*, 2, 1-27.
- Michelmores, T.R., 1971: The Geology of Copper Mineralized Areas in the
Olary Province. *Unpub. Hons. Thesis, Univ. of Adelaide*.
- Mookherjee, A., and Philip, R., 1979: Distribution of Copper, Cobalt and
Nickel in Ores and Host-Rocks, Ingladhal, Karnataka, India.
Mineral. Deposita, 14, 33-55.
- Orville, P.M., 1975: Stability of Scapolite in the System Ab-An-NaCl-
CaCO₃ at 4 kb and 750°C. *Geochim. Cosmochim. Acta*, 39, 1091-1105.
- Parker, A.J., 1972: A Petrological and Structural Study of a Portion of
the Olary Province West of Wiperaminga Hill, S.A.
Unpub. Hons. Thesis, Univ. of Adelaide.
- Plimer, I.R., 1977: The Origin of the Albite-rich rocks enclosing the
Cobaltian Pyrite Deposit at Thackaringa, N.S.W., Australia.
Mineral. Deposita, 12, 175-187.
- Plimer, I.R., 1978: Proximal and Distal Stratabound Ore Deposits.
Mineral. Deposita, 13, 345-353.
- Plimer, I.R., and Finlow-Bates, T., 1978: Relationship between Primary
Iron Sulphide Species, Sulphur Source, Depth of Formation and Age
of Submarine Exhalative Sulphide Deposits. *Mineral. Deposita*, 13,
399-410.
- Robertson, R.S., 1972: A Petrological and Structural Study of a portion of
the Olary Province West of Wiperaminga Hill, S.A.
Unpub. Hons. Thesis, Univ. of Adelaide.
- Schwartz, G.M., 1951: Classification and Definitions of Textures and
Mineral Structures in Ores. *Econ. Geol.*, 46, 578-591.
- **
Senior, A., and Leake, B.E., 1978: Regional metasomatism and the Geochemistry
of the Dalradian Metasediments of Connemara, Western Ireland.
J. Petrol., 19(3), 585-625.
- Skippen, G., 1974: An Experimental Model for Low Pressure Metamorphism
of Siliceous Dolomitic Marble. *Am. J. Sci.*, 274(5), 487-509.

- Spry, A., 1969: *Metamorphic Textures*. Pergamon Press, Oxford.
- Stanton, R.L., 1964: Mineral Interfaces in Stratiform Ores. *Trans. Inst. Mining Metall.*, 74(2), 45-79.
- Vokes, F.M., 1969: A Review of the Metamorphism of Sulphide Deposits. *Earth Sci. Review*, 5, 99-143.
- Waterhouse, J.D., 1971: The Geology of the Ethudna and Walparuta Mine Areas, Olary Province, S.A. *Unpub. Hons. Thesis, Univ. of Adelaide*.
- Wiltshire, R.G., 1975: The Structural Geology of the Old Boolcoomata Area, South Australia. *Unpub. Ph.D. Thesis, Univ. of Adelaide*.
- Winkler, H.G.F., 1979: *Petrogenesis of Metamorphic Rocks*. 5th Edition, Springer-Verlag, New York Inc.
- *Compston, W., and Arriens, P.A., 1968: The precambrian geochronology of Australia. *Can. J. Earth Sci.*, 5, 561-583.
- Compston, W., Crawford, A.R., Bofinger, V.M., 1966: A radiometric estimate of the duration of sedimentation in the Adelaide Geosyncline, South Australia. *J. Geol. Soc. Aust.*, 13, 229-276.
- **Scott, S.D., 1974: Sulphide Mineralogy. Editor P.H. Ribbe, Mineralogical Society of America Short Course Notes.

APPENDIX I

REPRESENTATIVE ROCK DESCRIPTIONS

T.S. Thin section
P.T.S. Polished thin section
P.S. Polished section

A. REPRESENTATIVE THIN SECTION DESCRIPTIONS

(i) Calc Silicate Horizon

Sample 764.211 T.S.

Feldspar 60%

Actinolite 20%

Epidote 8%

Hornblende 8%

Trace-calcite, sphene, apatite

Poorly layered; predominantly xenoblastic feldspar, oligoclase An₂₆. Both dusty and recrystallized feldspars occur. Actinolites form large laths ~1.5 mm with ragged boundaries. Fine grained hornblende <0.2 mm occurs in layers associated with epidote, which forms granular aggregates. Minor calcite as alteration product. Sphene and apatite accessories.

Sample 764.68 P.T.S.

Pyrite 35%

Feldspar 25%

Actinolite 25%

Epidote 15%

Traces-apatite, sphene, jarosite

Banding is evident (i) pyrite-rich horizon, (ii) epidote-actinolite, (iii) feldspar-rich horizon. Feldspars are fine grained, xenoblastic. Actinolite, as large radiating aggregates up to 3 mm, with some zoning evident. Fine grained opaques along cleavage planes of actinolite. Epidote occurs as disseminated grains or as granular aggregates with pyrite and actinolite. Large euhedral pyrite, ~2 mm which partially altered to melnikovite pyrite.

Sample 764.37 P.T.S.

Feldspar	60%
Augite	25%
Hornblende	7%
Sphene	5%

Trace-pyrite, sphalerite, biotite, apatite, epidote.

Poorly banded. Mainly xenoblastic, zoned, poikiloblastic feldspars average ~0.5 mm. Also large xenoblastic augite up to 2 mm. Hornblende, alteration rims on the augite, with sphene and opaques seemingly as alteration products also. Opaques are fine grained ≤ 0.2 mm and xenoblastic.

Sample 764.385 T.S.

Andradite	60%
Quartz	15%
Hedenbergite	13%
Calcite	10%

Massive, coarse, subeuhedral andradites up to 5.5 mm. Calcite-quartz-hedenbergite occurs interstitially as medium grains ~1 mm. Calcite and quartz appear to be alteration products of the hedenbergite, with lobate grain boundaries suggesting textural disequilibrium.

(ii) The Mixed Horizon

Sample 764-DR 6 T.S.

Calcite	50%
Tremolite	32%
Pyrite	15%
Biotite	3%

Poorly developed fabric. Large tremolite grains <3 mm, with biotite found in fractures. Intimate association between tremolite-calcite; both probably retrograde alteration products, showing textural disequilibrium. Calcite grain boundaries poorly developed, and show variation in grain size. Fine grained pyrite found along cleavage directions of calcite and tremolite.

Sample 764.212 T.S.

Feldspar	55%
Epidote	25%
Actinolite	8%
Biotite	6%
Quartz	4%

Trace-sphene, chlorite, apatite

Sample 764.212 (cont'd)

Dominated by recrystallized feldspar, average 0.1 mm, but larger dusty, zoned strained feldspars occur interstitially ~0.9 mm. Epidote as skeletal aggregates in feldspar horizon, but is coarser grained in the epidote-actinolite-biotite rich layers. Minor chlorite alteration of biotite and actinolite.

Sample 764.CR10A P.T.S.

Biotite	38%
Quartz	30%
Epidote	30%
Pyrite	2%

Trace-zircon, apatite, sphene, jarosite.

Banding defined by variation in grain size and composition.

(i) Biotite-rich horizons with zircon, (ii) biotite-quartz-epidote bands which are fine grained ~0.2 mm; epidote is zoned and forms granular aggregates, (iii) quartz-epidote bands which are fine grained. Some recrystallized coarse grained quartz ribbons. Pyrites euhedral ≤ 1 mm and concentrated in biotite-rich layers. Biotites ~1 mm define the schistosity which is parallel to banding.

Sample 764.63 P.T.S.

Calcite	30%
Scapolite	22%
Diopside	20%
Quartz	20%
Opaques	5%

Trace-clinozoisite, sphene.

Poikiloblastic diopside and scapolite ~2 mm, with inclusions of quartz and calcite; grain boundaries lobate. Fine grained calcite and quartz 0.1-0.2 mm interstitial to diopside-scapolite. Large recrystallized polygonal calcite <2 mm predominates. The fine grained calcite is alteration product of diopside, along with opaques which occur along the cleavage planes of diopside. Scapolite is mottled in appearance; sphene associated with it.

Sample 764.111 P.T.S.

Quartz	35%
Epidote	25%
Calcite	15%
Diopside	10%
Pyrite	10%
Actinolite	5%

Trace-sphene, goethite.

Sample 764.111 (cont'd)

Banding defined by grain size. (i) coarse grained quartz-epidote-diopside-calcite. (ii) fine grained quartz-epidote-calcite actinolite layers. Diopside up to 1 mm, have actinolite rims and calcite as alteration products along cleavage planes. Some calcite coarse grained ~1.0 mm and twinned, occurring with granular epidote aggregates <1.5 mm which are often flattened parallel to layering. Pyrite associated with epidote.

Sample 764.224 T.S.

Feldspar	45%
Epidote	30%
Biotite	20%
Muscovite	5%
Trace-apatite	

Fine grained mosaic of xenoblastic feldspar-epidote with micas defining weak schistosity. Epidote 0.1-0.2mm forms reticulate texture or granular aggregates. Feldspar, oligoclase is fine grained, ≤ 0.15 mm; larger grains undulose and elongate parallel to schistosity. Biotite <0.2 mm. Muscovite is minor; associated with biotite.

Sample 764.387 T.S.

Actinolite	50%
Epidote	40%
Quartz	5%
Calcite	2%
Sphene	1%
Trace-opaques	

Actinolite-large poikiloblastic laths with calcite and quartz as alteration products. Opaque stringers along actinolite cleavage planes. Large euhedral sphenes, randomly distributed. Dominantly decussate mosaic of xenoblastic actinolite and epidote ~1 mm in size.

Sample 764.77 P.T.S.

Biotite	64%
Opauques	20%
Epidote	8%
Chlorite	4%
Apatite	2%
Zircon	2%

Trace-siderite, goethite

Sample 764.77 (cont'd)

Biotite schistosity and elongation of pyrite lenses parallel to layering define the fabric. Pyrites ~1.5 mm; some slightly fractured. Minor haematite, magnetite, ilmenite. Most biotite ≤ 1.0 mm, with opaque inclusions along cleavages; zircon inclusions in biotite. Chlorite alteration of biotite and opaques. Epidote forms fine grained aggregates. Minor boxwork development with goethite rims around siderite rhombs ~0.1 mm. Apatite, rounded and disseminated.

Sample 764.78A P.T.S.

Quartz	68%
Opaques	15%
Biotite	10%
Chlorite	5%
Epidote	2%
Trace-apatite	

Banding defined by grain size variation and is paralleled by biotite schistosity. Polygonal recrystallized quartz ~0.1 mm. A few coarse grained quartz ~0.5 mm which associated with pyrite-biotite-chlorite. Pyrite, porphyroblastic >2 mm, often fractured. Biotite ≤ 1.0 mm, defines weak schistosity; associated with opaques. Chlorite associated with biotite; fine grained. Epidote aggregates - minor. Apatite-rounded, randomly dispersed.

Sample 764.66 P.T.S.

Diopside	40%
Epidote	35%
Scapolite	20%
Opaques	5%
Trace-chlorite, sphene, apatite	

Weakly banded. Dominated by xenoblastic diopside-epidote with interstitial poikiloblastic scapolite. Epidote as aggregates; a few large grains up to 1.0 mm; often contain fine grained opaque inclusions; some epidote zoned with clinozoisite rims. Diopside poikiloblastic, equant ≤ 1.5 mm, associated with epidote and opaques. Scapolite large ≤ 3.0 mm, poikiloblastic, undulose. Minor opaques, pyrite and chalcopyrite; pyrite up to 2 mm or as small idiomorphic grains. Sphene and apatite random.

Sample 764.95 P.T.S.

Opagues	65%
Calcite	26%
Quartz	5%
Trace-goethite	

Pyrite porphyroblasts up to 4 mm; polygonal texture, probably recrystallized; minor sphalerite along grain boundaries. Calcite interstitial to pyrite; polygonal texture; twinned, large grains up to 2 mm. Minor quartz aggregates, recrystallized. Goethite alteration on rims of pyrite.

Sample 764.DR 21 T.S.

Calcite	30%
Quartz	20%
Tremolite	20%
Diopside	20%
Opagues	3%

Trace-sphene, phlogopite, feldspar, scapolite

Banding defined by grain size and compositional variation. Very fine grained quartz horizons interbedded with coarse grained calcite-tremolite-diopside-opagues. Diopside, large, poikiloblastic. Tremolite alteration of diopside, in places completely replaced the diopside. Tremolite, poikiloblastic ≤ 2 mm with calcite and quartz inclusions. Quartz mostly fine grained. Calcite, large ≤ 1.0 mm, or as fine grained alteration product. Minor phlogopite associated with tremolite and diopside.

Sample 764.54 P.T.S.

Calcite	25%
Biotite	20%
Quartz	20%
Opagues	15%
Epidote	15%

Trace-sphene, muscovite

Coarse banding defined by biotite-rich horizons and coarse grained calcite layers. Porphyroblastic development of epidote and pyrite. Epidote is frequently zoned. Biotite ≤ 1.0 mm. Fine grained quartz-epidote-mica interlayered with coarse grained calcite horizons. Quartz, mostly recrystallized, fine grained; larger, serrated grains occur. Pyrite disseminated through host.

Sample 764·CR 13 P.T.S.

Calcite	25%
Biotite	20%
Epidote	20%
Muscovite	15%
Quartz	10%
Opagues	10%

Banding due to mica-rich horizons and coarse grained calcite-epidote-opaques. Quartz overlaps the two horizons and is interstitial to both horizons. Calcite lenses length parallel to banding. Mica is fine grained, average 0.2 mm. Opaques (chalcopyrite >pyrite>pyrrhotite) are associated with epidote and calcite. Fabric defined by mica schistosity, elongation of quartz lenses and compositional banding.

(iii) The Quartz-Feldspar-Mica Horizon

Sample 764·LL 9 T.S.

Feldspar	50%
Muscovite	25%
Biotite	20%
Quartz	5%
Trace-opaques	

Very fine grained. Xenoblastic mosaic of feldspars ~0.1 mm. These dusty and partially sericitized; occur interstitial to micas. Both muscovite and biotite (phlogopite?) occur. Maximum birefringence suggests phlogopite, these fine grained ~0.1 mm; define the schistosity. Muscovite ~0.2 mm, define schistosity. Phlogopite-rich bands occur. Small granular aggregates of opaques.

Sample 764.321 T.S.

Feldspar	85%
Biotite	5%
Sphene	5%
Quartz	2%
Apatite	2%
Trace-calcite, epidote, opaques	

Granoblastic mosaic of fine grained feldspar and biotite. Show weak layering. Most feldspar zoned and twinned; fine grained ~0.1 mm. Both oligoclase and microcline recognized with oligoclase > microcline (3:1). Feldspars dusty in appearance. Biotite 0.1-0.2 mm; small needles. Sphene variable shape and form; aggregates ~0.2 mm, most <0.1 mm; rich red-brown colour, high Ti content. Apatite ~0.1 mm, random, rounded.

<u>Sample 764·CR 11</u>	<u>T.S.</u>
Quartz	45%
Opagues	20%
Biotite	15%
Muscovite	15%
Chlorite	5%
Trace-zircon, apatite	

Micas define the schistosity (fabric); frequently wrap around opaque porphyroblasts ~5 mm. Grain size variation in quartz; large ones show subgrain development, others fine grained recrystallized with polygonal texture. Chlorite alteration associated with micas. Zircon in biotite-rich layers.

(iv) Graphitic Metasiltstone

<u>Sample 764.236</u>	<u>T.S.</u>
Quartz	75%
Biotite	15%
Graphite	10%

Very finely laminated rock distinguished by graphite-rich and graphite poor horizons. Biotite develop parallel to this layering. Quartz-biotite, very fine grained <0.1 mm and graphite ≤.002 mm. Graphite, dusty grey grains. Coarser quartz horizons, graphite free.

B. REPRESENTATIVE POLISHED SECTION DESCRIPTIONS

<u>Sample 764·LL5</u>	<u>P.S.</u>
Pyrite	98%
Pyrrhotite	1%
Chalcopyrite	1%

Pyrites develop good triple point junctions with chalcopyrite at these junctions and along the pyrite grain boundaries. Pyrite ~1 mm; contain pyrrhotite inclusions; pyrite fragmented in part.

<u>Sample 764·LL6</u>	<u>P.S.</u>
Pyrite	85%
Haematite	15%
Trace-pyrrhotite, chalcopyrite	

Large pyrites > 2mm, extremely brecciated, explosive texture. These pyrites ~1.5 mm. Chalcopyrite-pyrrhotite-haematite rounded inclusions in pyrite. Chalcopyrite develops twinned faces. Pyrite grain boundaries lobate. Haematite-dusty, appears to have completely replaced magnetite.

Sample 764·LL 3 P.S.

Pyrite	96%
Chalcopyrite	3%
Pyrrhotite	1%

Massive pyrite horizon. Pyrite partially fragmented, and grain boundaries exhibit caries texture adjacent the gangue. Pyrrhotite as stringers in pyrite and along a few grain boundaries. Pyrite ≤ 2 mm.

Sample 764·LL10 P.S.

Pyrite	93%
Chalcopyrite	5%
Covellite	2%
Trace-magnetite, pyrrhotite	

Massive pyrite horizon with grains up to 3 mm. Often show caries texture adjacent to gangue. Large chalcopyrite along pyrite grain boundaries. Chalcopyrite partially replaced by covellite in a wedge shaped replacement. Pyrrhotite, chalcopyrite and magnetite inclusions in pyrite. Pyrite fractured with small splinters produced.

Sample 764·DR 9 P.S.

Pyrite	94%
Marcasite	5%
Chalcopyrite	1%
Trace-pyrrhotite	

Large pyrite grains up to 3 mm, with curvilinear grain boundaries. Partial alteration to melnikovite pyrite and marcasite. The melnikovite appears as a dusty surface on the pyrite in the initial stages of low T, retrograde alteration. Similarly, marcasite is alteration of pyrite; it forms a myrmekitic or graphic overgrowth on pyrite. The melnikovite occurs where the pyrite is brecciated.

Sample 764·CR 10 P.S.

Pyrite	90%
Sphalerite	10%

Band of large pyrites with a skeletal texture, occurring interstitial to gangue. They have very ragged grain boundaries and contain hair-line fractures. Sphalerite has very ragged interstitial appearance, because of its low form energy. Occurs as small interstitial grains containing lots of gangue inclusions.

<u>Sample 764·DR 25</u>	<u>P.S.</u>
Pyrrhotite	85%
Chalcopyrite	10%
Pyrite	5%
Trace-arsenopyrite	

Pyrrhotite varies from being massive to randomly disseminated grains. Wedges of pyrite occur in the pyrrhotite. Both chalcopyrite and pyrite form inclusions in the pyrrhotite. Chalcopyrite forms aggregates up to 2 mm, most ≤ 1.5 mm.

APPENDIX II

TRACE ELEMENTS IN PYRITE

Introduction

23 samples were chosen, which were found to be free of contamination by other sulphide material. This was determined by examining polished sections of the mineralization. Fresh samples of the pyrite were obtained from the D.D.H's LL1, CR1, DR4 and the MP wells. Of these 23 samples only 16 yielded enough pyrite concentrate for trace element determination. These 16 samples came from the following locations:

Sample Number	Location	Depth (metres)
764.LL1	DDH Lady Louise	32.5 - 32.55
.LL7	"	120.8 - 120.85
.LL8	"	120.95- 120.98
.CR4	DDH Cathedral Rock	92.1 - 92.23
.CR11	"	120.4 - 120.5
.CR14	"	133.4 - 133.5
.DR5	DDH Dome Rock	184.1 - 184.12
.DR8	"	193.83- 193.85
.DR9	"	195.45- 195.48
.DR10	"	197.1 - 197.15
.36	MP 3	80- 81
.65	MP 4	95- 96
.67	"	97- 98
.75	MP 5	29- 30
.78	"	32- 33
.96	MP 6	29- 30

Preparation of Pyrite Samples

All the samples were crushed using the Semi-micro Pulverizer. The powders were passed through a 120 mesh sieve, with the larger fraction being retained for study. These samples were washed in tapwater, with the fine grained suspension of clays and mud being removed. Most samples needed five washes to remove the fine grained suspension. The samples were then dried.

The samples were then separated using the Frantz Isodynamic Magnetic Separator, by increasing the amperage so that pyrite-silicate separation occurred. The last fraction of pyrite was separated using the heavy liquid, Tetra-bromo ethane (TBE). The result was pure pyrite with 1-2% contamination of silicates.

Pyrite Digestion

1. 1.0 or 0.5 gms of sample pyrite were weighed into a glass beaker, depending on the amount of pyrite concentrate produced.
2. 20 mls Aqua Regis and 2 mls Bromine were added to the sample.
3. This was heated at 70°C for the first hour and at 100°C for the second hour, and then evaporated to dryness (overnight).
4. 10 mls concentrated HCl and 10 mls distilled water were added to the cooled precipitate.
5. This was heated at 70°C for approximately one hour, or until all precipitate had dissolved.
6. Samples were cooled and made up to volume, 100 mls or 50 mls depending on the amount of original sample.

Trace Element Determinations

The solutions were determined for trace elements using the Philips Techtron AA6, by the atomic absorption method. The trace elements determined were Cu, Pb, Zn, Co, Ni, Bi, Cr, Mn, Sn, V and Ag. The results were determined by calibrating the values against standards. In the case of Bi, Cr, Sn and V, the values obtained were below the detection limit, so that an arbitrary low value was used to determine the maximum value.

The optimum operating conditions for AA determinations were:

Element	λ	I (mA)	SBP (nm)	PM (v)	I (H ₂)	Flame
Cu	324.8	3	0.5	393	3.2	Air-C ₂ H ₂
Pb	217	10	1.0	445	1.2	Air-C ₂ H ₂
Zn	213.9	6	1.0	416	1.5	Air-C ₂ H ₂
Co	240.7	7	0.5	418	1.7	Air-C ₂ H ₂
Ni	232	7	0.5	389	2.8	Air-C ₂ H ₂
Bi	223.1	8	0.5	432	-	Air-C ₂ H ₂
Cr	357.9	5	0.2	410	-	N ₂ O-C ₂ H ₂
Mn	279.5	5	0.5	339	5.2	Air-C ₂ H ₂
Sn	235.6	10	0.5	384	-	N ₂ O-C ₂ H ₂
V	318.7	15	0.1	355	-	N ₂ O-C ₂ H ₂
Ag	328.1	3	0.2	290	-	Air-C ₂ H ₂

The following table contains all the trace element determinations, including the values which have been included in the text as Table 1.

TRACE ELEMENTS IN PYRITE (PPM)

	Cu	Pb	Zn	Co	Ni	Mn	Ag	Sn*	Bi*	Cr*	V*
764.LL1	40	<5	760	2	29	<1	2	<38	<10	<4	<25
.LL7	1160	<5	55	30	60	5	3	<38	<10	<4	<25
.LL8	1230	<5	20	670	44	<1	2	<38	<10	<4	<25
.CR4	205	<5	45	20	39	<1	8	<38	<10	<4	<25
.CR11	2150	40	440	630	670	85	3	<38	<10	<4	<25
.CR14	580	130	260	570	440	72	4	<38	<10	<4	<25
.DR5	240	<5	10	1710	45	2	2	<38	<10	<4	<25
.DR8	70	<5	7	23	10	17	2	<38	<10	<4	<25
.DR9	70	<5	10	20	14	115	3	<38	<10	<4	<25
.DR10	40	<5	10	14	5	37	3	<38	<10	<4	<25
.36	6000	80	30	1000	135	1	2	<38	<10	<4	<25
.65	455	<5	6100	70	21	72	4	<38	<10	<4	<25
.67	1970	<5	1050	240	135	20	4	<38	<10	<4	<25
.75	23	<5	90	150	50	38	3	<38	<10	<4	<25
.78	75	265	275	100	50	56	4	<38	<10	<4	<25
.96	29	<5	50	24	22	17	2	<38	<10	<4	<25
Average	896	34	576	330	110	34	3	<38	<10	<4	<25
Range	23-6000	<5-265	7-6100	2-1710	5-670	<1-115	2-8	<38	<10	<4	<25

*Denotes below the limit of detection by A.A. Values are arbitrary maxima.

APPENDIX III

ANALYTICAL TECHNIQUES

I. SAMPLES FOR WHOLE ROCK ANALYSES

a. Sample Preparation

- (1) All weathered material was removed from the samples before crushing.
- (2) Samples were reduced to less than 1 cm in size, using the jaw crusher.
- (3) These fragments were ground to approximately 200 mesh in the Siebtechnik Chrome-steel Mill.

b. Whole Rock Oxide Analyses

- (1) Approximately 5 gms of the milled sample was heated at 900°C for 12 hours in a furnace, to determine the loss of volatiles (H₂O, CO₂, SO₂).
- (2) 0.28 gms of the ignited sample was mixed with 0.02 gms of sodium nitrate and 1.5 gms of lithium fluoride flux.
- (3) These were mixed thoroughly before being fused into buttons.
- (4) The oxide percentages of SiO₂, Al₂O₃, Fe₂O₃, MnO, MgO, CaO, K₂O, TiO₂ and P₂O₅ were determined using the fused buttons in the Siemens Sequential Ray Spectrophotometer, programmed with a digital tape.

c. Na₂O Determinations

- (1) Approximately 30 mgs of ignited powder was digested in a teflon beaker using 10 mls HF and 2 mls H₂SO₄.
- (2) The solutions were heated overnight at a temperature ~90°C or until all the HF had boiled off.
- (3) Most samples were made up to 100 ml volumes, but samples high in Na₂O, were made up to 250 mls. These were 764.17, 764.27, 764.44, 764.221, 764.224, 764.236, 764.254, 764.262 and 764.321.
- (4) The solutions were individually calibrated against known standards and the internal standard Black Hill Norite II, using the Corning EEL flame photometer.

d. Sulphur Determinations

- (1) 0.25 gms of unignited milled sample was mixed with approximately 0.9 gms of both tin and iron accelerator chips, in a special ceramic vessel.
- (2) The samples were fused in the Leco Induction Furnace for 6 minutes.

d. Sulphur Determinations (cont'd)

(3) The SO_2 given off, was collected and titrated against a burette containing a known concentration of KIO_3 . The titration was proportional to the concentration of KIO_3 used.

e. Carbon Dioxide Determinations

The method for CO_2 determination is similar to sulphur, except that the liberated CO_2 is collected in a sealed vessel and the increase in weight of the vessel each time is proportional to the CO_2 collected. The SO_2 liberated is absorbed by manganese dioxide granules before reaching the sealed vessel.

f. H_2O Determinations

(1) The total loss of volatiles was determined when the milled samples were ignited.

(2) The proportion of H_2O is equal to
Total loss on ignition - ($\text{CO}_2 + \text{S}$) for each sample.

II. TRACE ELEMENT ANALYSES

a. Sample Preparation

The same sample preparation procedure is used as in Ia.

b. Using Philips XRF Machine

(1) Approximately 5 gms of unignited rock powder was pressed into pellets using a 4psi. pressure.

(2) Only Tungsten(W) was measured using the XRF.

(3) All samples were determined for tungsten.

(4) Operating conditions:

Molybdenum tube; 60KV; 40mA

Li F220 crystal

Flow proportional counter in vacuum

Fine collimator

1 x 100 second count

(5) Lines measured:

W background angle 61.77°

W peak angle 62.57°

c. Using Siemens S.R.S.

(1) Barium-Scandium-Titanium contents were determined, using the pressed pellets.

(2) The values were obtained on the Siemens SRS using a digital tape programme.

d. Using the Atomic Absorption Method

- (1) 1.0 gms of unignited sample was placed in a teflon beaker with 2 mls conc. HClO_4 and 10 mls 50% HF.
- (2) These were heated on a teflon coated hotplate at $\sim 100^\circ\text{C}$ for 12 hours or until it boiled dry.
- (3) 10 mls of conc. HCl and a few mls distilled water were added to the cooled precipitate.
- (4) The samples were heated gently until all the crystals dissolved.
- (5) All samples were made up to 100 ml. volume.
- (6) All solutions were analysed for Cu, Pb, Zn, Co and Ni using the Varian Techtron A.A.6.
- (7) The operating conditions for each lamp were as follows:

Element	λ	I (mA)	SBP (nm)	PM (v)	I (H_2)	Flame
Cu	324.8	3	0.5	377.8	3.2	Air- C_2H_2
Pb	217	10	1.0	445.7	1.3	Air- C_2H_2
Zn	213.9	6	1.0	417	1.7	Air- C_2H_2
Co	240.8	7	0.5	415.7	1.7	Air- C_2H_2
Ni	232	7	0.5	384.3	3.2	Air- C_2H_2

APPENDIX IV

GEOCHEMICAL TABLES

TABLE 1: CALC SILICATES

	764.3	764.8	764.77	764.111	764.220	764.259	764.371
SiO ₂	63.40	29.82	38.59	39.78	55.21	48.95	58.97
Al ₂ O ₃	13.87	7.45	8.6	8.48	4.15	8.88	14.75
Fe ₂ O ₃	4.25	31.28	24.20	7.82	2.03	6.38	6.12
MnO	.08	.20	2.3	.46	3.44	3.70	.05
MgO	.53	4.59	2.33	2.44	.88	2.96	1.33
CaO	4.14	7.6	3.45	19.9	16.97	22.17	5.94
Na ₂ O	1.99	.57	.63	1.29	.15	.20	3.06
K ₂ O	8.28	2.13	3.54	2.22	.10	.58	6.52
TiO ₂	.48	.37	.42	.38	.13	.40	.56
P ₂ O ₅	.23	.18	.17	.19	.14	.41	.21
H ₂ O ⁺	1.04				1.81	.21	.39
CO ₂	.20	8.13	11.4	10.56	12.63	5.0	.78
S	.11	7.8	3.67	4.04	.06	.02	.01
Subtotal	98.60	100.12	99.30	97.56	97.69	99.86	98.68
Pb	4	6	38	152	27	85	0
Zn	71	223	5373	1256	748	260	27
Cu	17	2619	22	30	122	7	4
Co	30	36	103	30	32	16	26
Ni	24	49	84	26	22	8	27
Ba	5052	844	4277	12,756	5,587	1,021	3,063
Sc	12	7	27	9	5	6	15
W	430	262	208	288	210	336	314
Total	99.16	100.52	100.31	99.01	98.37	100.03	99.03

N.B. Oxides in wt %

Trace elements in p.p.m.

TABLE 2: QUARTZ-FELDSPAR-MICA (QFM)

	764.17	764.20	764.51	764.88	764.248	764.323	764.401
SiO ₂	59.76	55.33	67.51	63.62	57.92	61.29	65.07
Al ₂ O ₃	19.63	15.35	9.62	16.68	20.53	13.94	18.5
Fe ₂ O ₃	5.71	10.34	3.59	5.07	5.11	7.11	3.99
MnO	.08	.10	.10	.10	.12	.44	.12
MgO	2.31	2.25	.67	2.75	2.05	1.56	2.49
CaO	.63	5.11	5.84	.59	.40	6.00	.52
Na ₂ O	1.37	1.74	.29	1.63	1.56	.86	.97
K ₂ O	7.54	3.43	6.05	5.55	9.16	6.51	4.76
TiO ₂	.72	.59	.36	.77	.71	.57	.86
P ₂ O ₅	.16	.52	.31	.18	.18	.22	.06
H ₂ O ⁺	1.76		.17	1.96	2.30	.94	2.08
CO ₂		1.14	2.58		.14		
S	.40	3.66	1.13	.79	.02		
Subtotal	100.07	99.56	98.22	99.69	100.19	99.44	99.42
Pb	10	38	36	192	42	88	19
Zn	88	977	46	1068	202	341	300
Cu	22	73	38	78	48	31	14
Co	22	41	61	79	29	42	29
Ni	26	46	18	49	29	22	14
Ba	668	340	2096	1266	1042	9730	876
Sc	20	17	5	16	19	13	29
W	382	179	891	1065	350	446	256
Total	100.19	99.73	98.54	100.07	100.37	100.51	99.57

N.B. Oxides in wt %

Trace elements in p.p.m.

TABLE 3: PYRITIC CALC SILICATE AND GRAPHITIC METASILTSTONE

	Pyritic calc silicate		Graphitic Metasiltstone
	764.26	764.64	764.236
SiO ₂	48.67	32.31	68.23
Al ₂ O ₃	9.87	5.05	17.11
Fe ₂ O ₃	3.19	12.63	.58
MnO	.28	.39	
MgO	2.92	5.81	1.31
CaO	18.45	17.11	.76
Na ₂ O	1.63	.47	7.55
K ₂ O	3.52	1.85	1.24
TiO ₂	.39	.19	.63
P ₂ O ₅	.29	.16	.10
H ₂ O ⁺	1.14		
CO ₂	8.04	12.12	.63 (carbon)
S	.52	9.02	.02
Subtotal	98.91	97.11	98.16
Pb	102	79	4
Zn	1042	2861	23
Cu	89	108	17
Co	26	47	23
Ni	19	19	3
Ba	1940	8762	499
Sc	4	6	11
W	179	450	269
Total	99.25	98.34	98.24

N.B. Oxides in wt %

Trace elements in p.p.m.

TABLE 4: FELDSPAR (ALBITE) RICH ROCK ± CALC SILICATES

	764.27	766.44	764.224	764.321
SiO ₂	59.03	59.63	61.18	64.15
Al ₂ O ₃	9.51	16.26	16.28	16.68
Fe ₂ O ₃	21.82	4.65	5.98	.45
MnO	.06	.03	.22	.02
MgO	.80	1.82	2.12	.96
CaO	2.26	1.85	6.13	.98
Na ₂ O	4.8	2.7	1.36	.47
K ₂ O	.41	9.71	4.00	14.18
TiO ₂	.37	.62	.66	.69
P ₂ O ₅	.2	.17	.31	.30
H ₂ O ⁺		.14	1.58	.56
CO ₂	.18	.3		
S	.4	1.15	.02	.04
Subtotal	99.84	99.03	99.84	99.48
Pb	0	6	52	35
Zn	32	202	84	76
Cu	344	326	4	3
Co	60	89	39	22
Ni	14	27	29	8
Ba	189	993	1240	1630
Sc	7	14	12	11
W	639	891	233	296
Total	99.97	99.28	100.01	99.69

N.B. Oxides in wt %

Trace elements in p.p.m.

TABLE 5: $\text{Ca}_2\text{O}/\text{Na}_2\text{O}$ AND $\text{Fe}_2\text{O}_3/\text{MnO}$ RATIOS

	$\text{Ca}_2\text{O}:\text{Na}_2\text{O}$	$\text{Fe}_2\text{O}_3:\text{MnO}$
A. 764.3	2.1	53
.8	13.3	156
.77	5.5	10.5
.111	15.4	17
.220	113.0	0.6
.259	110.8	1.7
.371	1.9	122
B. 764.27	0.5	364
.44	0.7	155
.224	4.5	27.2
.321	2.1	22.5
C. 764.26	11.3	11
.64	36.4	32
D. 764.17	0.5	71.4
.20	2.9	103
.51	20.1	36
.88	0.4	50.7
.248	0.3	42.6
.323	7.0	16.2
.401	0.5	33.3
E. 764.236	0.1	-

A. Calc silicates

B. Feldspar rich rock \pm calc silicate

C. Pyritic calc silicate

D. Quartz-feldspar-mica

E. Graphitic metasiltstone.

APPENDIX V

WORK DONE

- (1) Two weeks field work; studying field relations of the calc silicates.
- (2) 47 thin section descriptions;
48 polished section descriptions.
- (3) 17 Whole Rock Analyses.
- (4) 16 Trace Element Analyses on Pyrite.
- (5) Compilation of Trace Element Studies on the MP1-MP10 wells.